

# AN EXAMINATION OF POST-MORTEM HUMAN IRIS RECOGNITION

by

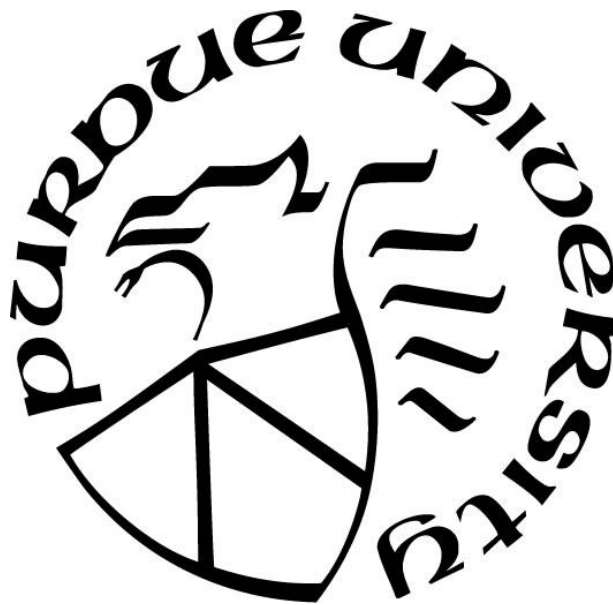
**Joseph Zweng**

**A Thesis**

*Submitted to the Faculty of Purdue University*

*In Partial Fulfillment of the Requirements for the degree of*

**Master of Science**



Department of Computer & Information Technology

West Lafayette, Indiana

December 2019

**THE PURDUE UNIVERSITY GRADUATE SCHOOL  
STATEMENT OF COMMITTEE APPROVAL**

Dr. Stephen J. Elliott, Chair

Department of Computer and Information Technology

Dr. Kathryn C. Seigfreid-Spellar

Department of Computer and Information Technology

Kevin J. O'Connor

Department of Technology Leadership & Innovation

**Approved by:**

Dr. Eric T. Matson

## ACKNOWLEDGEMENTS

I would like to thank a handful of people who provided knowledge, guidance, and assistance throughout the process of completing this thesis.

Firstly, my committee. Dr. Elliott guided me through my studies. He prompted the occasional overlooked questions at stuck points but more importantly, he encouraged me to push on when encouragement was essential. Dr. Seigfried-Spellar provided advice to help me get through the data collection process, a daunting task for me. Her expertise and enthusiasm about forensics turned an uncommon event into an adventure. Kevin O'Connor helped me through all aspects of my work. He has been a great individual to look up to and has become a great friend through this voyage.

Thank you to the coroners and staff who opened their doors and allowed me to work with them. Coroner Donna Avolt, for helping me explore the possibilities of this research and allowing me access to the coroner's facilities. And to Chief Deputy Coroner Alfie Ballew, for working on a tight schedule with me to complete data collections. All of the staff that I had the pleasure of working with, at both the Tippecanoe County Coroner's Office and the Marion County Coroner's Office, were extremely helpful. Their patience and understanding as I interrupted their daily work made the data collection process run smoothly.

To the rest of my support system, my family and friends. These are the people who have been by my side through this journey, cheering me on. For understanding the time commitment of completing this work and for the endless encouragement that I received.

I would also like to acknowledge the 15 subjects without whom, this research would not be possible.

# TABLE OF CONTENTS

|   |    |
|---|----|
| LIST OF TABLES .....                      | 7  |
| LIST OF FIGURES .....                     | 9  |
| ABSTRACT.....                             | 11 |
| CHAPTER 1. INTRODUCTION .....             | 12 |
| 1.1 Statement of the Problem .....        | 12 |
| 1.2 Significance of the Problem .....     | 12 |
| 1.3 Scope of the Study .....              | 13 |
| 1.4 Research Questions .....              | 13 |
| 1.5 Assumptions .....                     | 14 |
| 1.6 Limitations.....                      | 14 |
| 1.7 Delimitations .....                   | 14 |
| 1.8 Terms and Definitions .....           | 15 |
| CHAPTER 2. LITERATURE REVIEW .....        | 17 |
| 2.1 Introduction to Biometrics.....       | 17 |
| 2.2 Biometric Modalities .....            | 19 |
| 2.2.1 Biometrics in Law Enforcement.....  | 19 |
| 2.3 The Human Eye.....                    | 20 |
| 2.3.1 Vitrectomy Procedure.....           | 21 |
| 2.3.2 The Post-Mortem Eye .....           | 21 |
| 2.4 Forensic Sciences .....               | 22 |
| 2.4.1 Forensic Identification.....        | 23 |
| 2.4.2 Autopsy Procedures.....             | 23 |
| 2.5 Iris Recognition .....                | 24 |
| 2.5.1 History of Iris Recognition.....    | 25 |
| 2.5.2 Post-Mortem Iris Recognition .....  | 25 |
| 2.5.3 Iris Image Acquisition Process..... | 26 |
| 2.5.4 Image Processing.....               | 27 |
| 2.6 Iris Image Quality Metrics.....       | 29 |

|                              |   |    |
|------------------------------|---|----|
| 2.7                          | Iris Matching Performance .....         | 31 |
| CHAPTER 3. METHODOLOGY ..... |   | 34 |
| 3.1                          | Data Collection .....                   | 34 |
| 3.1.1                        | Population.....                         | 35 |
| 3.1.2                        | Subject Information.....                | 35 |
| 3.1.3                        | Testing Environment .....               | 36 |
| 3.1.4                        | Image Capture Process .....             | 36 |
| 3.2                          | Analysis of the Data .....              | 38 |
| 3.2.1                        | Image Quality Analysis .....            | 38 |
| 3.2.2                        | Performance Analysis.....               | 39 |
| 3.3                          | Threats to Validity .....               | 39 |
| CHAPTER 4. RESULTS .....     |   | 40 |
| 4.1                          | Subject Demographics .....              | 40 |
| 4.1.1                        | Subject 1 Data Summary .....            | 43 |
| 4.1.2                        | Subject 2 Data Summary .....            | 44 |
| 4.1.3                        | Subject 3 Data Summary .....            | 46 |
| 4.1.4                        | Subject 4 Data Summary .....            | 47 |
| 4.1.5                        | Subject 5 Data Summary .....            | 49 |
| 4.1.6                        | Subject 6 Data Summary .....            | 50 |
| 4.1.7                        | Subject 7 Data Summary .....            | 52 |
| 4.1.8                        | Subject 8 Data Summary .....            | 53 |
| 4.1.9                        | Subject 9 Data Summary .....            | 55 |
| 4.1.10                       | Subject 10 Data Summary .....           | 56 |
| 4.1.11                       | Subject 11 Data Summary .....           | 57 |
| 4.1.12                       | Subject 12 Data Summary .....           | 59 |
| 4.1.13                       | Subject 13 Data Summary .....           | 60 |
| 4.1.14                       | Subject 14 Data Summary .....           | 62 |
| 4.1.15                       | Subject 15 Data Summary .....           | 63 |
| 4.2                          | Analysis of Image Quality .....         | 65 |
| 4.2.1                        | Iris Detection Confidence Analysis..... | 67 |
| 4.2.2                        | Iris Pupil Concentricity Analysis ..... | 69 |

|   |   |    |
|---|---|----|
| 4.2.3   | Iris Pupil Contrast Analysis.....         | 70 |
| 4.2.4   | Iris Radius Analysis.....                 | 72 |
| 4.2.5   | Iris Sclera Contrast Analysis .....       | 74 |
| 4.2.6   | Margin Adequacy Analysis .....            | 75 |
| 4.2.7   | Pupil Boundary Circularity Analysis ..... | 77 |
| 4.2.8   | Pupil to Iris Ratio Analysis .....        | 78 |
| 4.2.9   | Sharpness Analysis.....                   | 80 |
| 4.2.10  | Usable Iris Area Analysis.....            | 81 |
| 4.3   | Analysis of Matching Performance .....    | 83 |
| CHAPTER 5. CONCLUSIONS AND FUTURE WORK .....          |   | 85 |
| 5.1   | Conclusions .....                         | 85 |
| 5.1.1   | Image Quality .....                       | 85 |
| 5.1.2   | Performance.....                          | 86 |
| 5.2   | Future Work.....                          | 86 |
| APPENDIX A. INSTITUTIONAL REVIEW BOARD EXEMPTION..... |   | 88 |
| APPENDIX B. PERFORMANCE DET CURVES .....              |   | 89 |
| REFERENCES .....                                      |   | 94 |

## LIST OF TABLES

|  |    |
|--|----|
| Table 2.1: Image Quality Levels.....   | 29 |
| Table 3.1: Conditional Setting for the Eye .....                                   | 35 |
| Table 3.2: Data Collection Tools .....   | 36 |
| Table 3.3: Conditions used for Analysis.....                                       | 38 |
| Table 4.1: Distribution of Subject Gender .....                                    | 40 |
| Table 4.2: Distribution of Subject Cause of Death .....                            | 40 |
| Table 4.3: Data Collection Table .....   | 42 |
| Table 4.4: Failure to Acquire Attempt Summary .....                                | 43 |
| Table 4.5: Subject 1 Images.....   | 43 |
| Table 4.6: Subject 2 Images.....   | 45 |
| Table 4.7: Subject 3 Images.....   | 46 |
| Table 4.8: Subject 4 Images.....   | 48 |
| Table 4.9: Subject 5 Images.....   | 49 |
| Table 4.10: Subject 6 Images.....  | 51 |
| Table 4.11: Subject 7 Image .....  | 52 |
| Table 4.12: Subject 8 Images.....  | 54 |
| Table 4.13: Subject 9 Images.....  | 55 |
| Table 4.14: Subject 10 Images.....   | 56 |
| Table 4.15: Subject 11 Images.....   | 58 |
| Table 4.16: Subject 12 Images.....   | 59 |
| Table 4.17: Subject 13 Images.....   | 61 |
| Table 4.18: Subject 14 Images.....   | 62 |
| Table 4.19: Subject 15 Images.....   | 64 |
| Table 4.20: Descriptive Statistics of Image Quality by Condition .....             | 65 |
| Table 4.21: Image Quality Examples by Condition.....                               | 66 |
| Table 4.22: Descriptive Statistics of Iris Detection Confidence by Condition ..... | 68 |
| Table 4.23: Descriptive Statistics of Iris Pupil Concentricity by Condition.....   | 69 |
| Table 4.24: Descriptive Statistics of Iris Pupil Contrast by Condition .....       | 71 |

|  |    |
|--|----|
| Table 4.25: Descriptive Statistics of Iris Radius by Condition.....                | 72 |
| Table 4.26: Descriptive Statistics of Iris Sclera Contrast by Condition .....      | 74 |
| Table 4.27: Descriptive Statistics of Margin Adequacy by Condition .....           | 75 |
| Table 4.28: Descriptive Statistics of Pupil Boundary Circularity by Condition..... | 77 |
| Table 4.29: Descriptive Statistics of Pupil to Iris Ratio by Condition.....        | 78 |
| Table 4.30: Descriptive Statistics of Sharpness by Condition .....                 | 80 |
| Table 4.31: Descriptive Statistics of Usable Iris Area by Condition .....          | 81 |
| Table 4.32: Matching Performance Summary .....                                     | 83 |

## LIST OF FIGURES

|   |    |
|---|----|
| Figure 2.1: Generic Model (Wayman, 1997).....   | 18 |
| Figure 2.2: Schematic Diagram of the Human Eye (Rhcasilhos & Jmarchn, 2007) .....     | 21 |
| Figure 2.3: Segmented Iris Capture .....  | 28 |
| Figure 2.4: Common Iris Capture Issues: Occlusion (left), Blurring, and Rotation..... | 28 |
| Figure 2.5: Similarity Score Histogram .....  | 33 |
| Figure 3.1: IriShield USB MK2120U Device.....   | 37 |
| Figure 4.1: Histogram of Subject Age .....  | 41 |
| Figure 4.2: Subject 1 Match Score Boxplot by Condition.....                           | 44 |
| Figure 4.3: Subject 2 Match Score Boxplot by Condition.....                           | 45 |
| Figure 4.4: Subject 3 Match Score Boxplot by Condition.....                           | 47 |
| Figure 4.5: Subject 4 Match Score Boxplot by Condition.....                           | 48 |
| Figure 4.6: Subject 5 Match Score Boxplot by Condition.....                           | 50 |
| Figure 4.7: Subject 6 Match Score Boxplot by Condition.....                           | 51 |
| Figure 4.8: Subject 7 Match Score Boxplot by Condition.....                           | 53 |
| Figure 4.9: Subject 8 Match Score Boxplot by Condition.....                           | 54 |
| Figure 4.10: Subject 9 Match Score Boxplot by Condition.....                          | 56 |
| Figure 4.11: Subject 10 Match Score Boxplot by Condition.....                         | 57 |
| Figure 4.12: Subject 11 Match Score Boxplot by Condition.....                         | 58 |
| Figure 4.13: Subject 12 Match Score Boxplot by Condition.....                         | 60 |
| Figure 4.14: Subject 13 Match Score Boxplot by Condition.....                         | 61 |
| Figure 4.15: Subject 14 Match Score Boxplot by Condition.....                         | 63 |
| Figure 4.16: Subject 15 Match Score Boxplot by Condition.....                         | 64 |
| Figure 4.17: Boxplot of Image Quality by Condition.....                               | 66 |
| Figure 4.19: Boxplot of Iris Detection Confidence by Condition .....                  | 68 |
| Figure 4.20: Boxplot of Iris Pupil Concentricity by Condition .....                   | 70 |
| Figure 4.21: Boxplot of Iris Pupil Contrast by Condition .....                        | 71 |
| Figure 4.22: Boxplot of Iris Radius by Condition .....                                | 73 |
| Figure 4.23: Boxplot of Iris Sclera Contrast by Condition.....                        | 74 |

|   |    |
|---|----|
| Figure 4.24: Boxplot of Margin Adequacy by Condition.....             | 76 |
| Figure 4.25: Boxplot of Pupil Boundary Circularity by Condition ..... | 77 |
| Figure 4.26: Boxplot of Pupil to Iris Ratio by Condition .....        | 79 |
| Figure 4.27: Boxplot of Sharpness by Condition.....                   | 80 |
| Figure 4.28: Boxplot of Usable Iris Area by Condition.....            | 81 |
| Figure A 1: IRB Human Subjects Research Exemption.....                | 88 |
| Figure B 1: DET Curve: Condition 1 vs Condition 1 .....               | 89 |
| Figure B 2: DET Curve: Condition 1 vs Condition 2a .....              | 89 |
| Figure B 3: DET Curve: Condition 1 vs Condition 2b .....              | 90 |
| Figure B 4: DET Curve: Condition 1 vs Condition 3 .....               | 90 |
| Figure B 5: DET Curve: Condition 2a vs Condition 2a.....              | 91 |
| Figure B 6: DET Curve: Condition 2a vs Condition 3 .....              | 91 |
| Figure B 7: DET Curve: Condition 2b vs Condition 2b .....             | 92 |
| Figure B 8: DET Curve: Condition 2b vs Condition 3 .....              | 92 |
| Figure B 9: DET Curve: Condition 3 vs Condition 3 .....               | 93 |

## **ABSTRACT**

This research focused on the evaluation of iris recognition on post-mortem subjects. It was to determine if iris image captures were suitable from post-mortem subjects and if the captures contained the features required to be used in recognition scenarios. One commercially available iris camera was used, the IriShield USB MK2120U. In order to complete this research, it was first necessary to obtain images from subjects that contain the proper features, including sharpness, pupil size, and image quality. The images were captured during three different conditions that would be possible to find under real-world circumstances. The first condition was as the decedent came into the coroner's office before the vitreous fluid was sampled from the eyes. The second condition was after the vitreous fluid was sampled from the deceased. Sampling vitreous fluid is a common autopsy procedure. This second condition would also be similar to a subject with a punctured eye. The third condition was after replacing the volume of vitreous fluid with saline solution. Replacing the vitreous with saline restored the round shape to the eye. This study found that high quality images can be captured from a post-mortem eye and that matching images across conditions results in positive identification.

# CHAPTER 1. INTRODUCTION

In the field of biometrics, the topic of iris recognition after death has not been heavily researched (Sauerwein, Saul, Steadman, & Boehnen, 2017; Trokielewicz, Czajka, & Maciejewicz, 2016, 2019). In the first of his two papers, Trokielewicz studied the ability to identify individuals in a mortuary setting over a time period after death. This study showed that it was possible to capture iris images from the deceased and that the images were able to be recognized by commercially available matching systems. Another paper showed similar results, that the iris images of deceased individuals were able to be identified by a commercially available matcher. In this study however, the subjects were located in an uncontrolled environment where decomposition of the bodies occurred naturally (Sauerwein et al., 2017). None of the existing papers, however, have examined the ability of a commercially available matcher to identify individuals after an autopsy procedure.

This chapter will give an overview of the research performed regarding post-mortem iris recognition during autopsy procedures. The chapter contains the statement of the problem, the significance of the problem, the scope of the study, the research questions, assumptions, limitations, delimitations, and terms and definitions.

## 1.1 Statement of the Problem

The purpose of this study was to investigate the suitability of iris recognition use on deceased individuals from the perspective of image quality and performance. This included three conditions; before, during, and after autopsy procedures.

## 1.2 Significance of the Problem

The use of biometric systems, including iris recognition, has become mainstream. Iris recognition implementations exist in a number of environments, including healthcare, finance, automotive, retail and personal devices (Frost, 2017). The iris is a suitable candidate to use for recognition because each iris contains complex patterns with a high level of variability. The iris is also a part of the body that is considered to be stable over time, meaning that images taken

years apart have a high likelihood of a positive match (Daugman, 2009; Petry, 2015). The interest in researching post-mortem iris recognition arose primarily for forensics and law enforcement use. The primary uses for post-mortem iris recognition would be to identify an unknown decedent or verify the identity of a decedent. If an iris template for the individual had been previously enrolled, the individual would be able to be quickly identified or verified even if other identifiable features were not usable. While Trokielewicz has analyzed the performance of post-mortem iris recognition (Trokielewicz & Czajka, 2018; Trokielewicz et al., 2019), no studies had incorporated any autopsy procedures.

### 1.3 Scope of the Study

The purpose of this study was to determine the suitability of post-mortem iris recognition. A commercially available iris recognition device, the IriTech IriShield USB MK2120U and a commercially available image quality feature extraction and matching tool, Neurotechnology SDK 10, were used to capture images and process the matching results. Data for this study was collected at the Marion County Coroner's Office and the Tippecanoe County Coroner's Office during a single visit for each subject. During the visit, the iris camera was used to capture multiple images of each iris at multiple conditions. The device that was used for image acquisitions was the IriTech IriShield USB MK 2120U. The Neurotechnology SDK 10 was used to determine image quality metrics and perform matching. Image quality and matching performance were used to determine if post-mortem iris recognition is possible after autopsy procedures.

### 1.4 Research Questions

This study examined the following research questions:

- Can iris images of deceased adults be acquired from multiple conditions with acceptable quality?
- Can iris images of deceased human adults be matched between multiple conditions?
  - Condition 1: Images captured before vitreous has been sampled.
  - Condition 2a: Images captured after vitreous has been sampled, with no visible deflation of the eye.

- Condition 2b: Images captured after vitreous has been sampled, with visible deflation of the eye.
- Condition 3: Images captured after saline has replaced the vitreous fluid?

### 1.5 Assumptions

The assumptions for this research included the following:

- The lighting conditions of both of the data collection areas were controlled.
- There was no documented trauma to the eye prior to the start of the data collection.
- The IriTech IriShield USB MK 2120U iris camera is capable of capturing images on post-mortem irises as it is on living adult irises.
- Neurotechnology SDK 10 is able to process images of post-mortem irises as it is on living adult irises.

### 1.6 Limitations

The limitations for this research included the following:

- The time of death may be unknown.
- The subject pool was limited to the deceased located at the Marion County Coroner's Office and the Tippecanoe County Coroner's Office.
- The amount of vitreous sampled was unknown due to the operational nature of the coroner's offices and was not collected.
- Any moisture added to the eye could impact the ability to capture and was not collected.

### 1.7 Delimitations

The delimitations for this research included the following:

- Only a single capture device, the IriTech IriShield USB MK2120U, was used during this study.
- Only a single quality algorithm and matcher, Neurotechnology SDK 10, were used during this study.
- No other biometric modalities were collected during this study.

## 1.8 Terms and Definitions

**Biometrics:** “Biological and behavioral characteristics of an individual from which distinguishing, repeatable biometric features can be extracted for the purpose of biometric recognition (ISO 2017, p. 2).

**Biometric Feature Extraction:** “Process applied to a biometric sample with the intent of isolating and outputting repeatable and distinctive numbers or labels which can be compared to those extracted from other biometric samples” (ISO 2017, p. 10).

**Biometric Template:** “Set of stored biometric features comparable directly to probe biometric features” (ISO 2017, p. 6)

**Biometric Mated Comparison Trial:** “Comparison of a biometric probe and biometric reference from the same biometric capture subject. This has historically been referred to as ‘Genuine Trials.’” (ISO 2017, p. 19).

**Biometric Non-Mated Comparison Trial:** “Comparison of a biometric probe and biometric reference from different biometric capture subjects. This has historically been referred to as ‘Impostor Trials.’” (ISO 2017, p. 19).

**Cause of Death:** “Any injury or disease that produces a physiological derangement in the body that results in the death of an individual.” (Geberth, 2006, p. 632)

**Dilation:** “The ratio of the pupil radius to the iris radius” (Tabassi, Grother, & Salamon, 2011, p. 13).

**Enroll:** “Create and store a biometric enrolment data record in accordance with the biometric enrolment policy” (ISO 2017, p. 10)

**Failure to Capture:** “Failure of the biometric capture process to produce a captured biometric sample of the biometric characteristic of interest” (ISO 2017, p. 20).

**False Match Rate (FMR):** “Proportion of the completed biometric non-mated comparison trials that result in a false match” (ISO 2017, p. 21).

**False Non-match Rate (FNMR):** “Proportion of the completed biometric mated comparison trials that result in a false non-match” (ISO 2017, p. 21).

**Feature:** “Distinctive patterns such as arching ligaments, furrows, ridges, crypts, rings, corona, freckles, and a zigzag collarete” (Daugman, 2009, p. 716).

**Gaze Angle:** “The deviation of the optical axis of the subject’s iris from the optical axis of the camera” (Tabassi et al., 2011, p. 12).

Grey Scale Spread: “A properly exposed image with a wide and well distributed spread of intensity values” (Tabassi et al., 2011, p. 14).

Identification Mode: “The system recognizes an individual by searching the templates of all the users in the database for a match” (Jain, Ross, & Prabhakar, 2004).

Iris Pupil Contrast: “A measure of the image characteristics at the boundary between the iris region and the pupil” (Tabassi et al., 2011, p. 11).

Iris Sclera Contrast: “A measure of the image characteristics at the boundary between the iris region and the sclera” (Tabassi et al., 2011, p. 12).

Iris Shape: “The shape of the iris-sclera boundary” (Tabassi et al., 2011, p. 14).

Iris Size: “The number of pixels across the iris radius, when the iris boundary is modeled by a circle” (Tabassi et al., 2011, p. 14).

Match: Comparison decision stating that the biometric probe(s) and the biometric reference are from the same source” (ISO 2017, p. 7).

Motion Blur: “The blur caused by the motion of the camera, by the iris, or by both” (Tabassi et al., 2011, p. 15).

Pupil Shape: “A measure of regularity in pupil-iris boundary” (Tabassi et al., 2011, p. 12).

Quality: “A measure of the fitness of a biometric sample to accomplish or fulfill the biometric comparison decision” (ISO 2017, p. 21).

Saline Solution: “A solution of salt in water, especially one used medicinally or to keep contact lenses moist” (Collins, 2019).

Sharpness: “The absence of focus, blur” (Tabassi et al., 2011, p. 13).

Usable Iris Area: “The percentage of the iris that is not occluded by an eyelash, eyelid, specular reflections, or ambient specular reflections.” (Tabassi et al., 2011, p. 11).

Verification Mode: “The system validates a person’s identity by comparing the captured biometric data with their own biometric template(s) stored in the system database” (Jain et al., 2004, p. 1).

Vitreous Fluid: “Colorless, transparent, and gelatinous material that contacts the retina and helps hold it in place” (Garhart & Lakshminarayanan, 2016, p. 98).

## CHAPTER 2. LITERATURE REVIEW

This review of literature will cover the general concepts of biometrics and their use in law enforcement, structures of the human eye and deterioration of the structures of the eye after death, forensic sciences related to the research, iris recognition, iris biometric image quality metrics, and matching performance.

### 2.1 Introduction to Biometrics

Biometrics is the science of identifying individuals based on their characteristics (International Standard Organization, 2017). The word “biometrics” comes from the Latin root words of bio, meaning life, and metrics, indicating measurement. Put together, bio and metrics can be understood as measuring life. For a feature to be considered for use as a biometric it must contain the following characteristics, universality, distinctiveness, permanence, and collectability (Jain et al., 2004). The list of biometric modalities is numerous, including both physiological characteristics and behavioral characteristics. Some biometric modalities that are commonly used include fingerprint, face, hand geometry, iris, and signature.

Biometric systems are typically based on a generic model that contains five subsystems to describe the functions performed. The subsystems of the generic biometric model laid out by Wayman are data collection, transmission, signal processing, decision, and data storage (Wayman, 1997). Data collection is the presentation of the biometric to the sensor. This is the only step of the model that requires the human subject’s interaction with the capture device. If this is the users first time interacting with the system, then it is known as the enrollment to the system. Any subsequent interactions are either classified as either verifications or identifications (ISO, 2017). Transmission involves compressing the image, transferring and expanding it to the necessary output format. The image is then segmented to obtain the portion of the image that is relevant to the modality being used. Features are extracted from the segmented image during the signal processing phase. The image quality is scored during signal processing and is rejected if a pre-set threshold is not met. If the interaction is the user’s enrollment image, then the template is stored, otherwise the template is matched against previously enrolled templates. Finally, in the decision subsystem, the match is either accepted or rejected based on the matching threshold of

the system and the match score of the two templates. Data storage is a representation of how and where the images and templates are stored. Figure 2.1 shows the Mansfield and Wayman Generic Model.

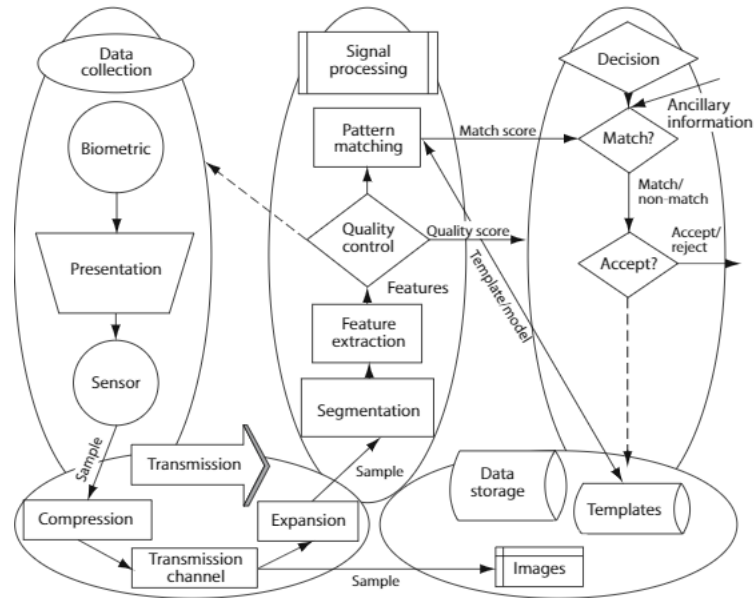


Figure 2.1: Generic Model (Wayman, 1997)

A biometric match can be one of two types of comparisons. The first comparison type is a genuine match or mated and is when the two templates being matched are from the same subject. An impostor match or non-mated is the second type of comparison and describes the attempted match of two templates from different subjects.

An attempted match, whether it is a mated or non-mated pair of templates, will generate a similarity score. The similarity score is a rating of the match and increases as the images are more similar. The similarity score is used when a threshold is set in place to give an accept or reject when the similarity score is over or under the predetermined threshold level. Four outcomes can be determined after a comparison is made. A match represents a mated pair whose similarity score is above the system threshold while a false non-match represents a mated pair whose similarity score is below the system threshold. Alternately, a false match represents a non-mated pair with a similarity score that is above the system threshold and a false non-match represents a non-mated pair with a similarity score that is below the system threshold (ISO, 2017).

## 2.2 Biometric Modalities

There are a number of different biometric modalities that are studied and used for recognition purposes. The most common of these, in no particular order, are palm print, fingerprint, face, iris, voice, signature, and vein (Rzemyk, 2017). The ideal biometric should be universal, meaning that every individual should have that specific feature, and it should be able to be captured. The technology available and implementation setting may restrict some biometrics and make certain others be a better solution.

Palm print and fingerprint are very similar biometrics. They both utilize unique features of the skin on the palm or pads of the fingers and ridge and valley characteristics. The main difference in the two has been the adoption of them. Fingerprint has proven to be more collectible. The systems for capturing and processing images have been developed for use while palm print recognition is still done primarily by hand.

### 2.2.1 Biometrics in Law Enforcement

Biometrics have been used in law enforcement as long as they have been studied. In the United States, the FBI has been using fingerprinting as a form of recognition since 1924. In 1986, the FBI implemented the Automated Fingerprint Identification System, or AFIS, combining manual processes and automated processes into a computer database (Rzemyk, 2017).

Law enforcement and other tactical forces have used biometrics as an identification tool. A majority of their field operations utilize multimodal biometric devices. These devices aim to capture multiple biometrics of the same individual during one collection period. These biometrics are often fingerprint, face, and iris. Three devices that have been used in a tactical operational setting are the Fusion, HIIDE, and SEEK (Stracener, Matey, Faddis, & Maxey, 2013). The goal with these devices is to capture the three biometric modalities of a subject when they are contacted by the officer or soldier.

Fingerprint is a common biometric used by law enforcement after death. A standard fingerprint card can be used with an ink pad to capture the fingerprints of the deceased. If the fingerprints of the individual have become shriveled or wrinkled, water is injected underneath the skin to restore the contours of the finger. In certain cases, most common with floaters, the skin of the fingers can begin to slip from the hand. This is referred to as de-gloving. If this

happens, the skin can be removed from the hand and a technician can obtain the prints by “wearing” the skin (Geberth, 2006).

### 2.3 The Human Eye

The human eye is an organ protected by a series of bones and tissue. The main structures of the eye include the sclera, cornea, iris, pupil, lens and vitreous humor. A typical human adult eye is roughly 24 mm in vertical diameter by 25 mm in horizontal diameter. An average eye weighs about 7.5 grams (Garhart & Lakshminarayanan, 2016).

The external components of the eye are the sclera and the cornea (Remington, 2005). The sclera forms the main structure of the eye and generally determines the globe shape. The sclera is a connective tissue and is normally white in color. Age or disease may result in a colored sclera while the sclera of newborn infants often appears bluish in color. Blood vessels run visibly through the sclera, but it is considered avascular because no capillary beds are present in it. The cornea is continuous with the sclera and is positioned at the front of the eye. The cornea is transparent, allowing for the best conditions for light transfer to the inner structures of the eye (Remington, 2005).

The vitreous humor, lens, and iris are the main interior components of the eye. The vitreous humor fills the eye and helps it to keep the round globe shape. It is a gelatinous liquid made up of mostly water. There are approximately 4.5 ml of vitreous humor in an eye, making up approximately 80% of the total volume of the eye (Lund-Andersen, Sebag, Sander, & La Cour, 2005). In some medical procedures, a portion of the vitreous humor must be removed. The process of removing the vitreous humor is called a vitrectomy and will be explained in the following section. The iris is the moving aperture of the eye that allows the correct amount of light to pass to the pupil and then on to the lens (Garhart & Lakshminarayanan, 2016). The iris is the component of the eye that is commonly used in biometric systems and can be a wide range of colors. Figure 2.2 shows the components that make up the human eye.

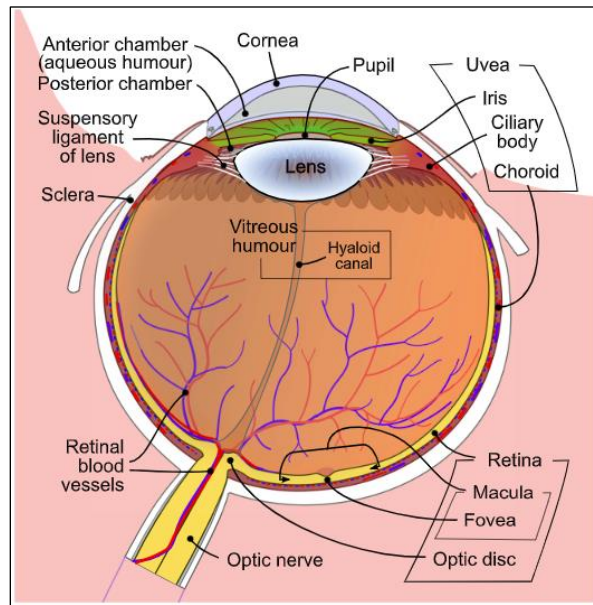


Figure 2.2: Schematic Diagram of the Human Eye (Rhcasilhos & Jmarchn, 2007)

### 2.3.1 Vitrectomy Procedure

A vitrectomy is a surgical procedure that involves removing a portion of the vitreous fluid. During a vitrectomy, the eye is entered through the sclera. The current methods of this procedure utilize extremely small surgical equipment that leaves self-sealing incisions approximately 0.5 mm in width. Vitreous humor is removed from the eye using a needle and syringe. The necessary procedures are completed and then the vitreous cavity is filled with either saline solution, a gas bubble, or silicone oil. The small incision heals without the need of sutures. The vitrectomy procedure is performed for a number of different reasons including opacity of the vitreous, retinal surgeries, for drug deliver, or for diagnostic purposes (American Society of Retina Specialists, 2016).

### 2.3.2 The Post-Mortem Eye

Changes to the eye after death can happen both naturally and with human intervention. The pupil will not respond to light stimulants after death. Typically, when the eyelids are closed, the eye will be more resistant to changes because it is protected from the elements. The elements that cause the most change to the eye include the temperature, humidity, and wind of the surrounding environment.

Natural changes to the eyes after death are the cornea becoming cloudy and the surface of the eye drying out. The cornea, or clear film over the iris, sometimes becomes cloudy within minutes after death (Geberth, 2006). If the cornea is cloudy, then the iris would not be visible. The surface of the eye will dry out after death, especially if the eye is open.

Changes that happen to the eye from human intervention can be from the cause of death (COD), first responder's actions or from common autopsy procedures. The cause of death also creates many possible changes to the eye. Trauma during or after death can cause the eye to be punctured or hemorrhaged from pressure. The position that the body is in after death also causes changes to the eye. If the body is in a facedown position, lividity will cause the blood to pool and result in petechial hemorrhaging (Geberth, 2006).

First responders can also cause change to the eye after death. The dilation of the pupil in response to illumination is used as a sign of death. A first responder will typically open the eye to check for pupillary response to light, which would indicate life. If the responder does not close the eyelids, then they will remain open leaving the eye exposed to the elements (Geberth, 2006).

Autopsy procedures result in the final change to the eye after death. Sampling vitreous for toxicology is a practice that occurs during the autopsy (Bévalot, Cartiser, Bottinelli, Fanton, & Guitton, 2016). When the vitreous is removed from the eye, the outer walls of the eye fall in similar to a deflated ball.

## 2.4 Forensic Sciences

Forensic science is the examination of evidence from crime scenes to help an investigation (United States DOJ, 2019). Forensic sciences encompass many scientific methods and disciplines that are used during criminal investigations. The goal of forensics is to analyze evidence and interpret the evidence to be presented in a legal manor or written in a report (James, Nordby, & Bell, 2014). For any investigation that a forensic scientist is involved in, they will use the data that is available to them to form a justification about the case. Forensic sciences are used throughout the analysis of crime scene evidence. This section will focus on methods of identification used for decedents and the procedures of autopsies performed by pathologists.

### 2.4.1 Forensic Identification

If an unknown decedent is found, it can be the task of the forensic scientist to identify the body. There are multiple methods that are used for identification. One method is the inspection of items that are found with the decedent. These items could be a wallet with an ID card, the registration of a vehicle or any other identifiable items. A relative can also formally identify a body. More technical methods of identification include fingerprinting, DNA tests, and odontology. Collecting fingerprints from a body can be a delicate task. Skin slippage can occur from decomposition or from the hand being submerged in water. If this occurs, the fingertips can be inflated with water or the skin can be removed and “worn” by the investigator. DNA samples can be collected from the individual and dental x-rays can be acquired to compare to known samples. Both of these methods require extensive equipment and can be time consuming processes (Geberth, 2006). Numerous other methods exist to identify decedents.

### 2.4.2 Autopsy Procedures

Forensic pathology, a section of forensic medicine, focuses on the examination of deceased individuals. An autopsy is the examination performed to determine the cause of death. During the autopsy, forensic pathologists act as an unbiased medical experts to assist in the determination of the cause and manner of death (Eriksson, 2016). Commonly, autopsies are performed when the cause of death is unusual, which can be natural, accidental, suicide, homicide, or undetermined (Skelton, Marsh, & Woods, 2001).

The first portion of an autopsy is an external exam. During the external exam, general observations of the body are recorded. The position of the body should be documented along with any fluids around the body. Clothing is documented and then removed. Additional information that is recorded is descriptors of the body, items that are attached to the body, any modifications, signs of injury or disease, and signs of decomposition. Photos are also taken of the body from head to toe. The documentation can be completed as notes accompanied with a body diagram indicating the position of any features. The order that the steps of an external exam are completed in is not significant (Suvarna, 2016).

Samples are collected for toxicology following the external exam. Some samples can be collected before the evisceration while others can only be collected during or after the

evisceration. Vitreous humor, blood, and urine can be collected before the evisceration begins. To collect vitreous, a needle is inserted as distally and as laterally as possible into the sclera of the eye. Between 2 and 3 ml of vitreous humor are typically collected. The eye can then be inflated with water. Toxicology of vitreous humor can be used to determine the levels of sodium, urea, creatinine, glucose, alcohol, cocaine and other substances. The collection of a blood sample is commonly completed with the use of a needle inserted into the femoral vein. Urine is also collected with the use of a needle that would be inserted above the symphysis pubis into the bladder. Blood and urine toxicology is used for microbiology assessments (Suvarna, 2016).

The third step of an autopsy is the evisceration. During the evisceration, the torso is opened, and tissue is removed. It is important to photograph the process. The order that evisceration is completed is important. The process begins by removing the organs from the mouth and works down to the anus. Fluid and tissue samples are collected throughout the process for later analysis. The organs are documented. Following the completed autopsy, the organs will be transported for further examination or placed back into the cavity of the body.

Not all cases require a full evisceration, some autopsies may be complete after the external exam. Even when a full evisceration is not needed, it is good practice to collect samples for toxicology.

## 2.5 Iris Recognition

Iris recognition is a biometric that utilizes the pattern of the iris as a unique identifying characteristic. Iris recognition, as a biometric is younger than other biometric modalities. The first patent for iris recognition was issued in 1987 and covered the methods for identifying a human eye on the basis of the visible features of the iris (Flom & Safir, 1987). The use cases of iris recognition are broad, as it can be used for computer login purposes, access control, surveillance and other identification purposes (Du, 2006). The iris is the colored part of the eye, bounded by the pupil on the inside and the white sclera on the outside (Jain et al., 2004). Iris recognition offers a high level of distinctiveness, also referred to as “within class variation”, meaning that the chance of finding two matching irises is very slim (Daugman, 2009). The high level of distinctiveness of the iris makes it a good candidate for biometric use, especially when used with large datasets and when false matches must be avoided. Daugman (2009) states that the iris is an internal organ and is stable over time yet is it visible externally, making data

collection relatively easy. It is stated, however, that the stability of the eye only lasts until a few minutes after death (Al-Raisi & Al-Khourri, 2008).

### 2.5.1 History of Iris Recognition

The observation that the human iris is a distinct feature dates to at least 1949, when James Doggart stated, “Just as every human being has different fingerprints, so does the minute architecture of the iris exhibit variations in every subject examined” (Doggart, 1949, p 27). The method of identifying an iris was first patented by Leonard Flom and Aran Safir in 1987 (U.S. Patent No. 4,641,349, 1987). In the patent, it is stated that iris recognition can be performed easily because the iris is visible. The advantages of utilizing the human iris over other biometrics, listed in the patent, are that tampering with the iris can be very dangerous and result in a loss of sight and that the images could be captured with little cooperation from the subject. The 1994 patent by Daugman illustrates the operational method of iris recognition. First capturing an iris image digitally, then segmenting the image to include only the necessary features, encoding the data, and finally matching to a previously enrolled sample (U.S. Patent No. 5,291,560, 1994). The operational method described in Daugman’s patent is still used as the backbone of iris recognition systems today.

### 2.5.2 Post-Mortem Iris Recognition

Only a small number of studies have collected images of post-mortem irises (Trokielewicz et al., 2016; Sauerwein et al., 2017; Trokielewicz et al., 2019). Some researchers have spoken about the ability, or inability, to use the iris for recognition after death. Al-Raisi & Al-Khori (2008) stated that the stability of the eye only lasts moments after death. This statement implies that any length of elapsed time would make it impossible to capture an image of the iris to be used for identification purposes. In a BBC interview, Daugman stated “Soon after death, the pupil dilates considerably, and the cornea becomes cloudy” (BBC News, 2001, p. 1). A dilated pupil would mean that the usable iris area would be considerably small while a cloudy cornea would obstruct the iris. Other researchers have shown that degradation of the iris does not occur minutes after death but rather hours and even days after death (Trokielewicz et al., 2016). The human body begins to deteriorate and decompose at the time of death. The eye will no longer

respond to illumination after death, meaning that the pupil will not dilate or contract as the pupil of a living subject would. Trokielewicz et al. (2016) found that after death, the pupil is at mid dilation and is fixed. The shape of the pupil is normally regular but past eye conditions of the individual can change this. In his first study, Trokielewicz was able to capture iris images starting 5-7 hours after death and then at regular time intervals for up to 27 hours after death.

A time study was conducted on post-mortem biometrics at the Anthropology Research Facility in Tennessee, USA. In this study, researchers left intact bodies to decompose naturally in an outdoor environment. They returned on a daily basis to capture images as the bodies decomposed. When returning to capture images of the iris, a sterile saline solution was used to hydrate the left eye, while the right eye remained untreated. The additional hydration of the left eye was found to have no effect on the longevity that the iris is viable for images. The results of this study concluded that while the season has a large impact on the decomposition of the body and also the different biometric features that were being examined. The researchers did find, however, that it is possible to capture feature rich images of the iris days after death (Sauerwein et al., 2017).

Certain characteristics of a post-mortem eye can influence the ability to capture a quality image of the iris. When the cornea becomes dry, it has a tendency to wrinkle and this can lead to poor images or failure to capture an image (Trokielewicz & Czajka, 2018). The second main issue is the cloudiness of the eye after death. The cornea of the eye can become cloudy starting just after death and will increase in opacity over time (Kawashima et al., 2014). If the opacity of the cornea becomes too high, then it could affect the ability to produce a quality iris image because it would occlude the iris.

### 2.5.3 Iris Image Acquisition Process

Iris recognition systems use methods to capture images that generally follow similar processes. The processes use a camera and a source of light, usually ambient and controlled illumination, to capture a raw image. The controlled illumination is commonly infrared because it is able to sufficiently illuminate the eye without causing discomfort to the subject (Daugman, 2009). A captured image of an iris is expected to contain at least 100 pixels in iris diameter, however a high quality sample is commonly over 200 pixels in iris diameter (JTC 1/SC 37,

2005). One issue during the capture process is subject movement, which can cause a blurred image or occlusion of the iris.

There are three main types of cameras that are used for iris recognition near infrared (NIR) cameras, high-resolution digital cameras, and telescopic iris cameras. NIR cameras perform up to 2 ft. from the subject and require a high level of subject cooperation. High-resolution digital cameras can take appropriate pictures for iris recognition but at an extremely close distance of just 2 inches. This can be very intrusive to the subject and also requires a high amount of subject cooperation. Finally, telescopic cameras can acquire high quality images from up to 10 ft away. Telescopic cameras do not require the same level of cooperation from the subject as NIR or high-resolution digital cameras do (Du, 2006).

#### 2.5.4 Image Processing

After an image of the iris is captured, the iris must be segmented from the surrounding features. The image may contain features of the eye including the pupil, sclera, tear duct, and surrounding tissue. These features must be segmented away, leaving only the usable portion of the iris. Segmentation is achieved by locating the pupillary boundary of the iris and the limbus (sclera) boundary of the iris. Figure 2.3 shows a segmented iris capture. The arrows indicate the pupillary boundary and the limbus boundary. The next step is to find the eyelid boundary with the iris. If over 50% of the iris is obstructed by the upper or lower eyelids, then the image is deemed inadequate and will be rejected (Daugman, 2009).

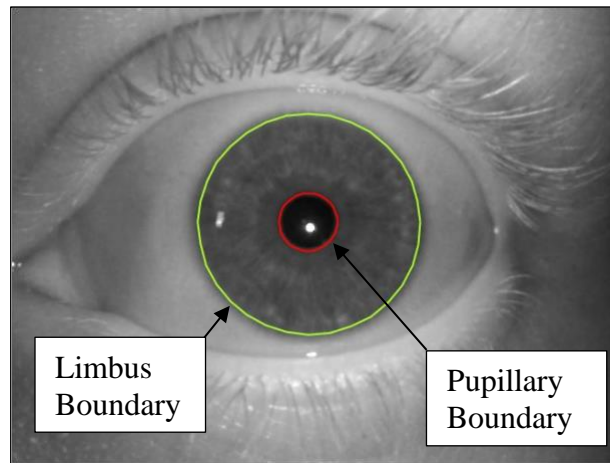


Figure 2.3: Segmented Iris Capture

If the image does not meet the quality threshold of the segmentation tool, then the image will not be able to be segmented. There are many issues that can result in an inability to segment an image. Some of the common issues are occlusion, out of focus images, orientation, and excessive pupil dilation (JTC 1/SC 37, 2005). Occlusion is the term that is used to describe an iris that is partially obstructed. Occlusion can be caused by a partially closed eyelid or eyelashes covering a portion of the iris. If the iris is occluded too much, it can become impossible to find the bounds of the iris, therefore making it impossible to segment the iris from the image (Bowyer, Hollingsworth, & Flynn, 2016). Figure 2.4 shows three poor iris images from left to right, an occluded iris, a blurred image, and a rotated orientation image.



Figure 2.4: Common Iris Capture Issues: Occlusion (left), Blurring, and Rotation

There are numerous factors that can have great effects on the performance of an iris recognition system. Pupil size is a factor that changes over time and is important to iris recognition. “Pupil size becomes smaller in an almost linear manner with increasing age” (Winn, Whitaker, Elliott, & Phillips, 1994, p 1135). The study by Winn et al. (1994) on pupil dilation

only included subjects with healthy eyes. It was determined that across five different illumination levels, the dilation of the pupil decreases with age. This is significant for iris recognition if a segmentation tool is optimized for a certain pupil size. If the age of the subject is known before the image capture, then the illumination could be adjusted to the optimal level for that subject for the best dilation. The sensor that is used can also be a factor of interest. Digital devices, including cameras, can be affected by use and time causing image quality to change (Bergmuller, Debiasi, Uhl, & Sun, 2014). While sensor aging does occur, it is more common that a sensor experiences extreme failure at some point, rather than a linear degradation of quality.

Image quality is determined by the different factors captured in the image. Some of the factors considered when determining image quality are the sharpness, the usable iris area, and the pupil to iris ratio. Image quality can be used to reject acquired images before they are matched to avoid poor matching performance.

Following segmentation, the iris image is transformed into iris code using 2D Gabor wavelet demodulation. This captures the “what” and “where” specific information about the iris is extracted (Daugman, 2009). This forms the template that can be used to enroll a user into a biometric system or match against a pre-existing enrolled template.

## 2.6 Iris Image Quality Metrics

The ability to capture samples with usable quality features is extremely important for a well performing system. High-quality iris images result in fewer matching errors than lower quality samples do (Tabassi et al., 2011). Iris image quality is rated on a scale of 0 - 100. The image is ranked poor, low, medium, or high depending on the rating of image quality shown in Table 2.1. Image quality is acceptable for matching when the quality value is greater than 50 (JTC 1/SC 37, 2005).

Table 2.1: Image Quality Levels

| <b>Image Quality Level</b> | <b>Image Quality Value</b> |
|----------------------------|----------------------------|
| Poor                       | 0 - 25                     |
| Low                        | 26 – 50                    |
| Medium                     | 51 – 75                    |
| High                       | 76 - 100                   |

The metrics used to determine the quality of iris images are the usable iris area, iris-sclera contrast, iris-pupil contrast, pupil boundary circularity, grey scale utilization, iris radius, pupil dilation, iris pupil concentricity, margin adequacy, and sharpness. An additional metric that Neurotechnology SDK 10 computes is the iris detection confidence. Tabassi, Grother, and Salamon (2011) summarize the meaning of each image quality metric and their importance to the overall quality of the image.

The usable iris area is described as the most important metric in determining the image quality score. The usable iris is determined to be the part of the iris that is visible in the image, unobstructed by any means. Common obstructions, known as occlusions, are the subject's eye lid or lashes and reflections. In the case that the occlusion is a result of the subject's eye lid or lashes, the occlusion cannot be reduced without intrusive actions. If the occlusion is due to reflections or other environmental factors, then design controls can be used to reduce or eliminate the occlusion. One designed control that many systems use is the requirement of the subject to remove glasses before the capture process. Related to the usable iris area is the iris size. Irises that are too big or too small can cause recognition failure. The iris size is measured as pixels across the iris when modeled by a circle (Tabassi et al., 2011).

The iris-sclera contrast is a measure that appears where the iris meets the sclera. A higher contrast score will give lower false non match rates. Fluctuations in the iris-sclera contrast can be due to subject specific characteristics or from external factors like lighting or camera type. The iris-sclera contrast can be improved by designing a better capture process or by using a better acquisition system.

Iris-pupil contrast is a measurement of the contrast at the boundary of the iris and the pupil. This metric is naturally more difficult to determine than the iris-sclera contrast because of the lower contrast between the pupil and the iris. The iris-pupil contrast score can be improved with a better acquisition system.

Pupil boundary circularity looks at the shape of the pupil. The information of the iris just around the pupil is extremely dense. This means that finding the boundary of the iris and pupil is very important so that the information rich iris can be properly extracted. If the pupil is segmented incorrectly, then the feature rich portion of the inner iris may be segmented out of the image. If the pupil boundary determined incorrectly, the result is worse performance.

Grey scale utilization is an indication of the saturation of light through the image. If the image is undersaturated then the result is a very dark image. Oversaturation results in a lighter image. Both undersaturation and oversaturation produce images with poor quality. It is important to have the correct lighting to achieve a properly exposed image with a wide range of intensity.

The iris radius is determined as the number of pixels across the iris. The iris boundary is modeled as a circle and if the iris radius is too big or too small the system will perform poorly. The pupil dilation is a similar measure to the iris radius. It is the measure of the size of the pupil in relation to the iris. Extreme values of dilation result in poor performance. Controlling the illumination of the image capture can control the level of dilation of the pupil.

Iris pupil concentricity is the measure of off-axis captures. If the gaze is away from the capture device, then the iris and pupil will not be concentric. It is best to minimize the gaze angle by using visual cues to guide the user to look at the capture device.

Margin adequacy is the measure of the distance that the iris is from the nearest edge of the image. Improper margin adequacy can occur if the device does not line up correctly with the subject or from improper cropping. A segmentation tool may be able to correct for poor margin adequacy.

Sharpness measures the amount of defocus that is present in the capture. Defocus can occur from improper depth of field or movement. Positioning of the subject is the most critical element for optimal sharpness and should be a design element of the capture device. Low sharpness results in performance errors.

The iris detection confidence, a measure designed into Neurotechnology SDK 10, is a quick reference to verify the presence of an iris in an image (Neurotechnology, 2019).

The performance metrics can be good indicators of how a set of images will perform when matching. The most important metrics, the usable iris area, iris-pupil contrast, and pupil boundary circularity may affect performance more than others. All of the metrics provide insight as to why certain images may perform better than others (Tabassi et al., 2011).

## 2.7 Iris Matching Performance

A biometric system matches captured templates against previously enrolled templates. If the ground truth of the acquired image and the enrolled template are from the same individual the two are known as a mated pair. A match made between a mated pair is known as a genuine

match. Inversely, if the ground truth of the acquired image and the enrolled template are from different individuals then the pair is known as a non-mated pair. The match between a non-mated pair is known as an impostor match. Performing a match between two images will generate a similarity score (ISO, 2017). Matching a set of data will result in a matching output.

There are four metrics that are commonly used to analyze the performance of a biometric system. These can be calculated from the similarity scores obtained from the matching output. The first two metrics are the false match rate (FMR) and the false non-match rate (FNMR). The FMR is the proportion of impostor matches that are falsely matched while the FNMR is the proportion of genuine attempts that are rejected. The equations below show the FMR (1) and the FNMR (2).

$$FMR = \frac{\# \text{ of impostor matches } \geq \text{ threshold}}{\text{Total \# of impostor matches}} \quad (1)$$

$$FNMR = \frac{\# \text{ of impostor matches } < \text{ threshold}}{\text{Total \# of impostor matches}} \quad (2)$$

The next two metrics represent an implementational setting by including the number of failed attempts, or FTA rate, in the equations. By including the failed number of attempts, you can show how a system performs not only with the images that it is able to capture but also with the transactions that failed to process in the system. The false accept rate (FAR) is the proportion of transactions that are falsely rejected. The false reject rate (FRR) is the proportion of transactions that are falsely accepted (Dunstone & Yager, 2009). The equations below show the FAR (3) and the FRR (4).

$$FAR = FMR * (1 - FTA) \quad (3)$$

$$FRR = FTA + FNMR * (1 - FTA) \quad (4)$$

When a set of images have been processed and matched, the genuine distribution and impostor distribution can be graphed to create a similarity score histogram. Figure 2.5 shows a similarity score histogram. The two distributions are the impostor and genuine matches. If the distributions overlap, then there will be a FMR, a FNMR or some combination of the two. If there is no overlap in the distributions, then the threshold can be placed between the two, resulting in no errors in the system.

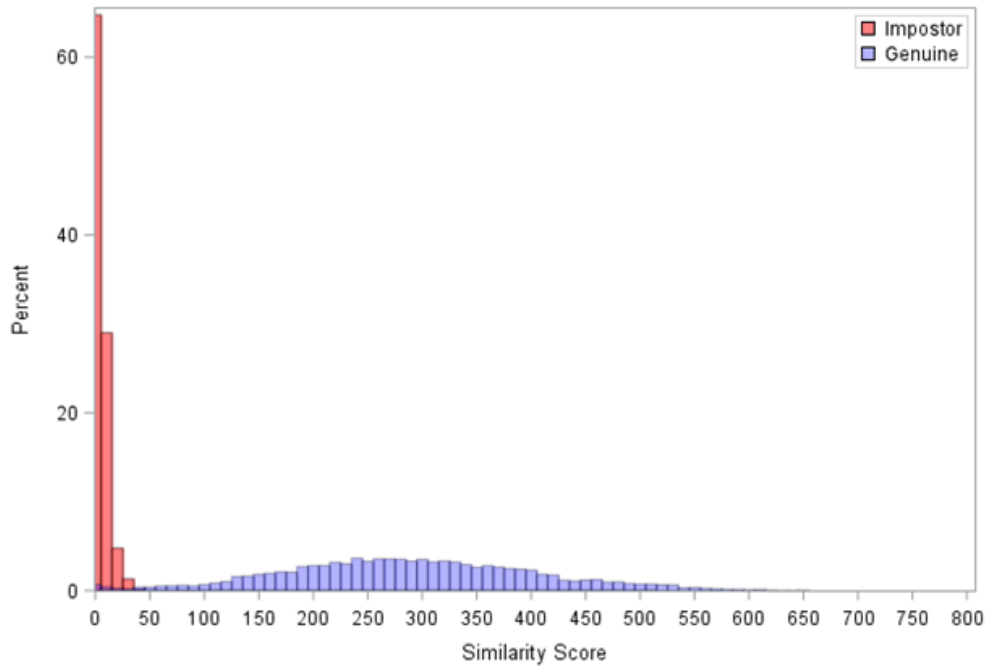


Figure 2.5: Similarity Score Histogram

The system performance can also be shown in a detection error tradeoff (DET) curve. This curve summarizes the system performance by plotting the false match rate against the false non-match rate (Dunstone & Yager, 2009). The DET curve will show the point at which the false accept rate and false reject rate are equal, which is known as the equal error rate (EER). It will also list the FAR at a selection of predetermined FRR's. This allows for a comparison of multiple different DET curves.

## CHAPTER 3. METHODOLOGY

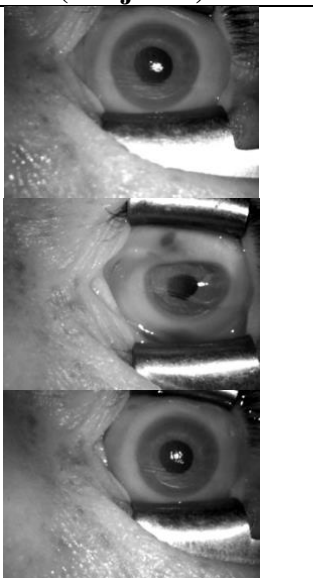
This chapter provides an overview of the procedures used to collect data for this research. It will also explain the analysis of the data.

### 3.1 Data Collection

The data collection for this research took place at the Marion County Coroner's Office and the Tippecanoe County Coroner's Office. The data collection was performed during a single visit for each subject. For each subject, iris images were acquired at three different conditions. For each condition, the eye was held open with ocular speculums or forceps.

The first data collection condition was before the vitreous humor was sampled from the eye. If any fluids or particulate were obstructing the eye, then cleaning would be completed. The pathologist would wipe the eye with a cloth or rinse the surface of the eye with saline. As Sauerwein (2017) found, the procedure of hydrating the eye, similar to rinsing, with a saline solution had no effect on the ability to capture images. The second condition was after vitreous fluid had been sampled from the eye. The removal of vitreous often caused the eye to deflate from the globe shape, however the amount of deflation was irregular. The third condition was after saline solution was injected into the eye until it inflated roughly to the dimension before vitreous was sampled. The addition of saline solution would reinstitute the natural shape of the eye. A summary of each condition along with an example of each can be found in Table 3.1. Appendix A contains the Institutional Review Board exemption for this study.

Table 3.1: Conditional Setting for the Eye

| Condition Number | Explanation of Condition   | Example of Condition (Subject 1)  |
|------------------|--|---|
| 1                | Before vitreous was sampled from the eye.                          |  |
| 2                | After the vitreous fluid is sampled from the eye.                  |   |
| 3                | With a volume of saline solution injected to replace the vitreous. |   |

### 3.1.1 Population

The population used for this study was a selection of the deceased from the Marion County Coroner’s Office and the Tippecanoe County Coroner’s Office. The selection of suitable subjects was chosen by the coroners based on characteristics involving the level of decomposition of the body and the cause of death. Anyone with visible or known trauma to the head were not selected for the study. The subjects also had to be over the age of 18. A total of 14 data collections were completed at the Marion County Coroner’s Office during six visits and one data collection was completed at the Tippecanoe County Coroner’s Office.

### 3.1.2 Subject Information

Demographic information and subject condition information was collected to aid in the interpretation of the data. This information included the age, sex, cause of death, and any other available information about the subject. Any outstanding notes or conditions of the subject were also recorded. Subjects were assigned a subject identification number that was used to save all images, but the name of the subject was not recorded.

### 3.1.3 Testing Environment

The testing environments used in this study were the Marion County Coroner’s Office and the Tippecanoe County Coroner’s Office. Subjects were kept in a temperature-controlled environment regulated at approximately 38 degrees Fahrenheit in both of the facilities. This environment is known to greatly reduce the rate of decomposition. Subjects were retrieved from the temperature-controlled room and brought into an examination room. The examination rooms were consistently lit by overhead fluorescent lighting. The temperature of the examination rooms was kept at approximately 70 degrees Fahrenheit. The temperature that a body is stored at is known to affect the rate of decomposition. The studies conducted by Trokielewicz et al (2016) utilized a hospital mortuary with the temperature controlled to approximately six degrees Celsius.

The images were captured as the pathologists were working on their case. In the operational setting during the autopsy, it was not possible to have unlimited capture attempts without causing major disruption to the workflow of the coroner’s office.

### 3.1.4 Image Capture Process

The tools used during the data collection are described in Table 3.2. The iris image captures were completed using the IriShield USB MK2120U device Figure 3.1. The images captured with this device adhere to ISO Standard 19794-6. The capture device was used to collect images of each iris during the three different conditions. Saline solution was used throughout the data collection process to rehydrate the surface of the eye if it became dry. This imitated the eyelids closing. All manipulations of the eyes were completed by a forensic pathologist or pathologist’s assistant.

Table 3.2: Data Collection Tools

| <b>Item Name</b>       | <b>Type</b>         |
|------------------------|---------------------|
| IriShield USB MK2120U  | Iris Capture Device |
| HP 2-in-1 Tablet       | Computer            |
| Neurotechnology SDK 10 | Software            |
| Ocular Speculum        | Autopsy Tool        |
| Forceps                | Autopsy Tool        |



Figure 3.1: IriShield USB MK2120U Device

It was not always possible to collect 5 images of each eye at each condition. If multiple failure to acquire occurred, then the software would be restarted, and the capture would be attempted again. If it became evident that an image would not capture, then the remaining images of that condition were skipped. The collection would continue with the remaining conditions.

The testing procedure was as follows:

1. The age, sex, cause of death, and any other notes were recorded for the subject; performed by the test administrator.
2. Ocular speculums were placed in the eyes to hold the eyes open; performed by a pathologist.
3. If necessary, a rag or saline solution was used to remove any particles from the surface of the eye. If the eye appeared dry, or if the device would not capture an image throughout the collection, then the saline solution was used to moisten the surface of the eye; performed by a pathologist.
4. Five images were captured of each eye using the IriShield USB MK2120U (Condition 1); performed by the test administrator.
5. Vitreous was sampled from the eyes; performed by a pathologist.
6. Five images were captured of each eye using the IriShield USB MK2120U (Condition 2); performed by the test administrator.
7. Saline solution was injected into the eye to replace the volume of vitreous fluid previously sampled from the eye; performed by a pathologist.

8. Five images were captured of each eye using the IriShield USB MK2120U (Condition 3); performed by the test administrator.

### 3.2 Analysis of the Data

The second half of the methodology is the analysis procedures. The images were first visually inspected. It was discovered that there was a range of deflation of the eye after the removal of the vitreous. Some of the images contained no visible signs of deflation while others were obviously deflated. Due to this fact, images from condition 2 were labeled as either 2a or 2b. Images were labeled “2a” if minimal deflation of the eye was visible after the vitreous was sampled. Images were labeled “2b” if there was obvious deflation of the eye visible in the images. This created 4 different conditions that were used for the analysis of image quality and matching performance, shown in Table 3.3. It should be noted that the process of designating images into group 2a or group 2b was completed visually and by a single researcher.

Table 3.3: Conditions used for Analysis

| <b>Condition Number</b> | <b>Explanation of Condition</b>   |
|-------------------------|---|
| 1                       | Before vitreous was sampled from the eye.   |
| 2a                      | After the vitreous fluid is sampled from the eye, and with no visible deflation of the eye. |
| 2b                      | After the vitreous fluid is sampled from the eye, and with visible deflation of the eye.    |
| 3                       | With a volume of saline solution injected to replace the vitreous.                          |

#### 3.2.1 Image Quality Analysis

The image quality was assessed using one-way ANOVA comparison of means statistical tests. Each quality metric was analyzed separately to determine if the condition had an effect on the metric. The quality score was the main measure to determine if images could be captured at each condition with usable quality. The remaining metrics were analyzed to further the understanding of what changes between each condition. Each analysis consisted of a one-way ANOVA comparison of means test and any necessary post-hoc tests.

### 3.2.2 Performance Analysis

The performance analysis was completed after matching between the conditions. The process of matching images was performed using Neurotechnology SDK 10. The output from matching the templates was processed using Oxford Wave Research Bio-Metrics 1.5. This tool allowed for the creation for detection error tradeoff curves (DET). The DET curves included the equal error rate (EER) and a set of false reject rates (FRR) at predetermined false accept rates (FAR). A total of 9 DET curves were created for the analysis. A lower EER indicated better performance.

### 3.3 Threats to Validity

The first threat to validity is selection bias. The methodology included adults who were deceased at the coroner's office without trauma. This included natural causes of death but not at a proportional rate as overdoses. A second threat to validity is researcher sampling variability. Many of the procedures used to manipulate the eyes were unconstrained and could introduce variability in the sampling. The variability of sampling could be due to the amount of vitreous removed from the eye or the amount of saline used to fill the eye. The iris device used is another threat to validity. The IriShield USB MK2120U is not a standardized device in operational settings.

## CHAPTER 4. RESULTS

This chapter reports the results of the study. The results are divided into the following sections: Subject Demographics, Image Quality and Matching Performance.

### 4.1 Subject Demographics

The subjects were chosen for the study based on criteria determined by the coroners. These criteria were that there was no known trauma to the head or eyes and the subject was over 18. The coroner also had the ability to not select a subject for the study for any other reason of their discretion. Each subject was assigned a unique subject identification number (SID) and data for the subject was denoted with “LE” for left eye and “RE” for right eye. Subject demographics were collected throughout the data collection. Table 4.1 shows the distribution of subject gender and Table 4.2 shows the distribution of the cause of death of the subjects. Figure 4.1 is a histogram of the age of the subjects. There were no specific demographic criteria required for subjects to be included in the study.

Table 4.1: Distribution of Subject Gender

| <b>Sex</b> | <b>Count</b> | <b>% of Total</b> |
|------------|--------------|-------------------|
| Female     | 4            | 26.7              |
| Male       | 11           | 73.3              |

Table 4.2: Distribution of Subject Cause of Death

| <b>Cause of Death</b> | <b>Count</b> | <b>% of Total</b> |
|-----------------------|--------------|-------------------|
| Accident              | 1            | 6.7               |
| Natural               | 3            | 20                |
| Overdose              | 11           | 73.3              |

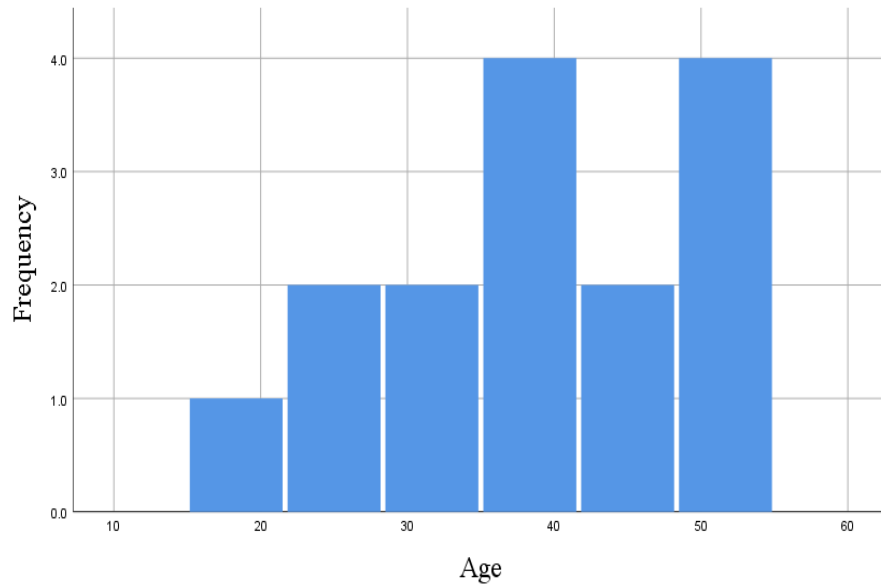


Figure 4.1: Histogram of Subject Age

The demographic information and notes of the data collection were recorded throughout the data collections. The complete data collection table is shown in Table 4.3. Included in the data collection table are the sex, age, cause of death, and number of images acquired for each subject.

Table 4.3: Data Collection Table

| SID | Date     | Sex | Age | Cause of Death | Eye | Images Captured per Condition |             |            |
|-----|----------|-----|-----|----------------|-----|-------------------------------|-------------|------------|
|     |          |     |     |                |     | Condition 1                   | Condition 2 | Condition3 |
| 1   | 10/8/19  | M   | 40  | Overdose       | LE  | 5                             | 1           | 5          |
| 1   |          |     |     |                | RE  | 5                             | 5           | 5          |
| 2   | 10/8/19  | M   | 24  | Overdose       | LE  | 5                             | 5           | 5          |
| 2   |          |     |     |                | RE  | 5                             | 5           | 5          |
| 3   | 10/9/19  | F   | 34  | Overdose       | LE  | 5                             | 5           | 5          |
| 3   |          |     |     |                | RE  | 5                             | 5           | 5          |
| 4   | 10/9/19  | M   | 32  | Overdose       | LE  | 5                             | 5           | 5          |
| 4   |          |     |     |                | RE  | 5                             | 5           | 5          |
| 5   | 10/10/19 | M   | 46  | Overdose       | LE  | 5                             | 5           | 5          |
| 5   |          |     |     |                | RE  | 5                             | 5           | 5          |
| 6   | 10/10/19 | M   | 38  | Natural        | LE  | 5                             | 5           | 5          |
| 6   |          |     |     |                | RE  | 5                             | 1           | 5          |
| 7   | 10/10/19 | F   | 52  | Overdose       | LE  | 5                             | 5           | 5          |
| 7   |          |     |     |                | RE  | 5                             | 5           | 5          |
| 8   | 10/14/19 | M   | 50  | Overdose       | LE  | 5                             | 5           | 5          |
| 8   |          |     |     |                | RE  | 5                             | 5           | 5          |
| 9   | 10/14/19 | F   | 51  | Overdose       | LE  | 5                             | 0           | 5          |
| 9   |          |     |     |                | RE  | 5                             | 5           | 5          |
| 10  | 10/14/19 | F   | 39  | Overdose       | LE  | 5                             | 5           | 5          |
| 10  |          |     |     |                | RE  | 5                             | 5           | 5          |
| 11  | 10/14/19 | M   | 28  | Overdose       | LE  | 5                             | 5           | 5          |
| 11  |          |     |     |                | RE  | 5                             | 5           | 5          |
| 12  | 10/14/19 | M   | 44  | Natural        | LE  | 5                             | 5           | 5          |
| 12  |          |     |     |                | RE  | 5                             | 5           | 5          |
| 13  | 10/16/19 | M   | 19  | Motor Vehicle  | LE  | 2                             | 3           | 1          |
| 13  |          |     |     |                | RE  | 3                             | 0           | 0          |
| 14  | 10/17/19 | M   | 36  | Overdose       | LE  | 5                             | 5           | 5          |
| 14  |          |     |     |                | RE  | 5                             | 5           | 5          |
| 15  | 10/17/19 | M   | 52  | Natural        | LE  | 5                             | 5           | 5          |
| 15  |          |     |     |                | RE  | 5                             | 5           | 5          |

During the data collections, five unique eyes experience failures to acquire. The attempts that were unable to be acquired are outlined in Table 4.4. The reason for the failures to acquire is not known but is discussed in the individual subject summary sections.

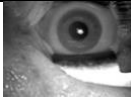
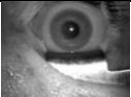
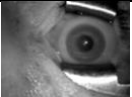
Table 4.4: Failure to Acquire Attempt Summary

| <b>SID/Eye</b> | <b>Cause of Death</b> | <b>Condition Missing</b> | <b>Observations</b> |
|----------------|-----------------------|--------------------------|---------------------|
| 1/LE           | Overdose              | 2                        | None                |
| 6/RE           | Natural               | 2                        | Jaundice            |
| 9/LE           | Overdose              | 2                        | Minor Decomp.       |
| 13/LE          | Motor Vehicle         | 1, 2, & 3                | 10 Day Coma         |
| 13/RE          | Motor Vehicle         | 1, 2, & 3                | 10 Day Coma         |

#### 4.1.1 Subject 1 Data Summary

Subject 1 was a 40-year-old male. His cause of death was an overdose. The forensic pathologist suspected that the individual used heroin. Table 4.5 shows the images captured of subject 1. The right and left eye images from condition 2 of subject 1 were all placed into group 2b as they showed obvious signs of deflation. Four attempts from the left eye at condition 2 were unable to capture for subject 1. The attempts that failed to acquire are indicated by “FTA” in Table 4.5. The FTA’s could be a result of the deformation of the eye when the vitreous was removed.

Table 4.5: Subject 1 Images

| <b>Eye and Condition</b> | <b>Capture Number</b>   |   |   |  |   |
|--------------------------|---|---|---|--|---|
|                          | <b>1</b>  | <b>2</b>  | <b>3</b>  | <b>4</b>   | <b>5</b>  |
| <b>LE 1</b>              |  |  |  |  |  |
| <b>LE 2</b>              |  | FTA   | FTA   | FTA  | FTA   |
| <b>LE 3</b>              |  |  |  |  |  |
| <b>RE 1</b>              |  |  |  |  |  |
| <b>RE 2</b>              |  |  |  |  |  |
| <b>RE 3</b>              |  |  |  |  |  |

The subject 1 match score boxplot in Figure 4.2 shows that the highest average genuine score for subject 1 was when condition 3 was matched to condition 3. All genuine performance that involved condition 2b was poor for subject 1.

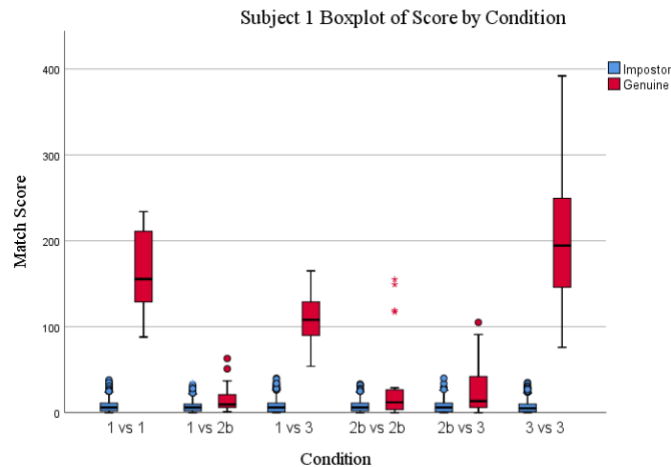


Figure 4.2: Subject 1 Match Score Boxplot by Condition

#### 4.1.2 Subject 2 Data Summary

Subject 2 was a 24-year-old male. His cause of death was an overdose. The coroner's notes indicated that the likely drug was methamphetamine. Table 4.6 shows the images captured of subject 2. Subject 2 did not experience any FTA's during the collection. The images of subject 2 from condition 2 were placed into group 2a because they did not show visible signs of deflation.

Table 4.6: Subject 2 Images

| Eye and Condition | Capture Number |   |   |   |   |
|-------------------|----------------|---|---|---|---|
|                   | 1              | 2 | 3 | 4 | 5 |
| LE 1              |                |   |   |   |   |
| LE 2              |                |   |   |   |   |
| LE 3              |                |   |   |   |   |
| RE 1              |                |   |   |   |   |
| RE 2              |                |   |   |   |   |
| RE 3              |                |   |   |   |   |

The subject 2 match score boxplot in Figure 4.3 shows that the highest average genuine score for subject 2 was when condition 2a was matched to condition 2a. This is interesting because it shows that good performance is possible if vitreous is removed but the eye is not visibly deflated. Matching images from subject 2 that included condition 1 was poor.

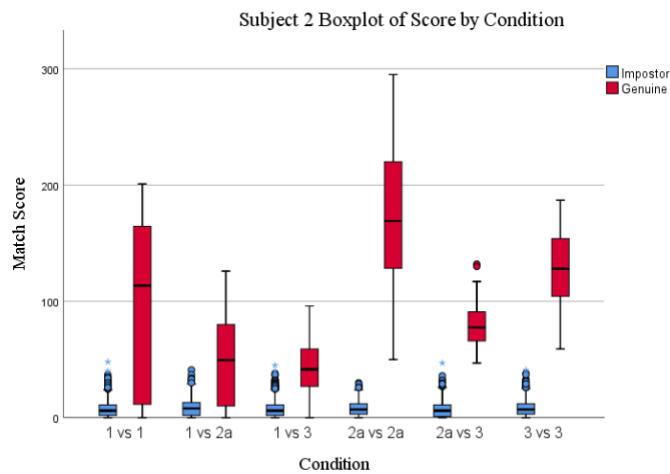


Figure 4.3: Subject 2 Match Score Boxplot by Condition

### 4.1.3 Subject 3 Data Summary

Subject 3 was a 34-year-old female. Her cause of death was an overdose. There was no indication of what substance the individual used. Subject 3 did not experience any FTA's during the collection. Table 4.7 shows the images captured of subject 3. The images of the left eye of subject 3 from condition 2 were placed into group 2b as they showed obvious signs of deflation after the removal of vitreous. The images of the right eye of subject 3 from condition 2 were placed into group 2a because they did not show obvious signs of deflation.

Table 4.7: Subject 3 Images

| Eye and Condition | Capture Number |   |   |   |   |
|-------------------|----------------|---|---|---|---|
|                   | 1              | 2 | 3 | 4 | 5 |
| LE 1              |                |   |   |   |   |
| LE 2              |                |   |   |   |   |
| LE 3              |                |   |   |   |   |
| RE 1              |                |   |   |   |   |
| RE 2              |                |   |   |   |   |
| RE 3              |                |   |   |   |   |

The subject 3 match score boxplot in Figure 4.4 shows that the highest average genuine score for subject 3 was when condition 1 was matched to condition 1. Lower genuine scores for subject 3 can be seen in the matching of condition 1 vs 2a, 1 vs 2b, and 2b vs 3.

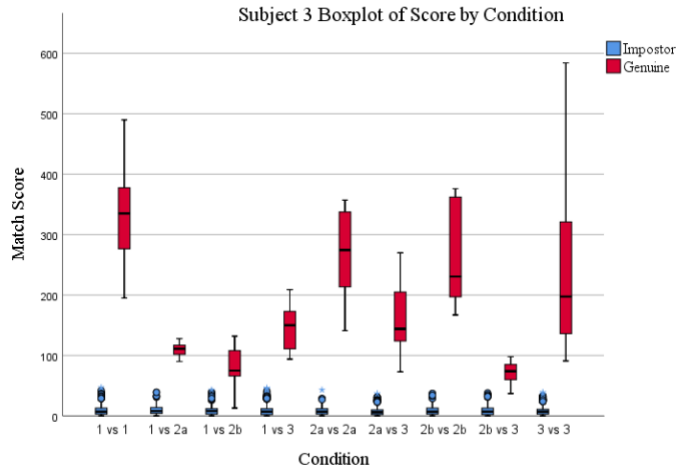


Figure 4.4: Subject 3 Match Score Boxplot by Condition

#### 4.1.4 Subject 4 Data Summary

Subject 4 was a 34-year-old male. His cause of death was an overdose. The subject was found with cocaine and there were indicators that other drugs were involved as well. Endotracheal intubation had been performed on the subject and the endotracheal tube was still in place. The subject had vomit and other fluids on his face that were wiped away by the pathologist's assistant. The eyes were then cleaned with saline solution prior to any image captures. Subject 4 did not experience any FTA's during the data collection. Table 4.8 shows the images captured of subject 4. All of the images of subject 4 taken during condition 2 were placed into group 2a because they did not show obvious signs of deflation.

Table 4.8: Subject 4 Images

| Eye and Condition | Capture Number |   |   |   |   |
|-------------------|----------------|---|---|---|---|
|                   | 1              | 2 | 3 | 4 | 5 |
| LE 1              |                |   |   |   |   |
| LE 2              |                |   |   |   |   |
| LE 3              |                |   |   |   |   |
| RE 1              |                |   |   |   |   |
| RE 2              |                |   |   |   |   |
| RE 3              |                |   |   |   |   |

The subject 4 match score boxplot in Figure 4.5 shows that the highest average genuine score for subject 4 was when condition 1 was matched to condition 1. Lower genuine scores for subject 4 can be seen in the matching of condition 1 vs 2a, 1 vs 3, and 2a vs 3.

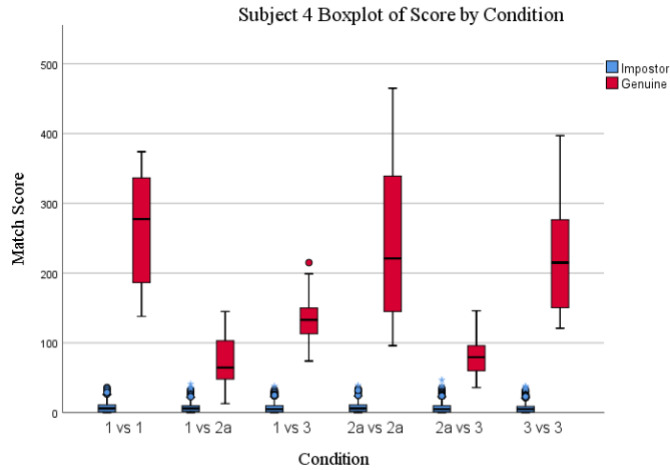
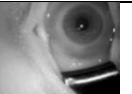
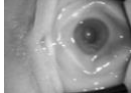
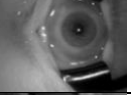
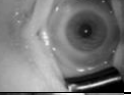
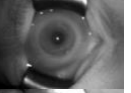
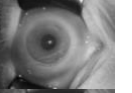
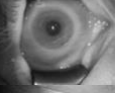
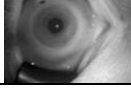
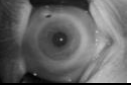
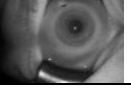
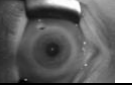


Figure 4.5: Subject 4 Match Score Boxplot by Condition

#### 4.1.5 Subject 5 Data Summary

Subject 5 was a 46-year-old male. His cause of death was an overdose. There was no indication of what substance the individual used. Table 4.9 shows the images captured of subject 5. All of the images of subject 5 captured during condition 2 were placed into group 2b, as they showed obvious signs of deflation after removal of vitreous.

Table 4.9: Subject 5 Images

| Eye and Condition | Capture Number  |   |   |   |   |
|-------------------|---|---|---|---|---|
|                   | 1   | 2   | 3   | 4   | 5   |
| LE 1              |    |    |    |    |    |
| LE 2              |    |    |    |    |    |
| LE 3              |    |    |    |    |    |
| RE 1              |   |   |   |   |   |
| RE 2              |  |  |  |  |  |
| RE 3              |  |  |  |  |  |

The subject 5 match score boxplot in Figure 4.6 shows that the highest average genuine score for subject 5 was when condition 3 was matched to condition 3. The lower genuine scores for subject 5 can be seen in the matching of condition 1 vs 2b and 2b vs 3.

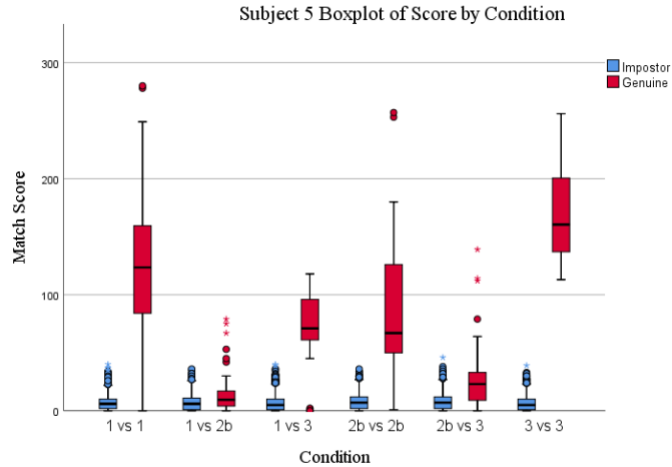


Figure 4.6: Subject 5 Match Score Boxplot by Condition

#### 4.1.6 Subject 6 Data Summary

Subject 6 was a 38-year-old male. His cause of death was determined to be natural, as there were no signs of drug use or foul play. The pathologist noted that the subject had severe jaundice, a condition that causes the whites of the eyes and the skin to become yellow. Table 4.10 shows the images captured of subject 6. Four images from the right eye at condition 2 were unable to capture for subject 6. The attempts that failed to acquire are indicated by “FTA” in Table 4.10. The first three images of the left eye of subject 6 from condition 2 were placed into group 2a as they did not show obvious signs of deflation. The fourth and fifth images of the left eye from condition 2 showed obvious signs of deflation and were placed into group 2b. The single image captured of the right eye during condition 2 was placed into group 2a as there were not obvious signs of deflation.

Table 4.10: Subject 6 Images

| Eye and Condition | Capture Number |     |     |     |     |
|-------------------|----------------|-----|-----|-----|-----|
|                   | 1              | 2   | 3   | 4   | 5   |
| LE 1              |                |     |     |     |     |
| LE 2              |                |     |     |     |     |
| LE 3              |                |     |     |     |     |
| RE 1              |                |     |     |     |     |
| RE 2              |                | FTA | FTA | FTA | FTA |
| RE 3              |                |     |     |     |     |

The subject 6 match score boxplot in Figure 4.7 shows that the highest average genuine score for subject 6 was when condition 1 was matched to condition 1. All of the genuine distributions when condition 2a or 2b were involved were poor.

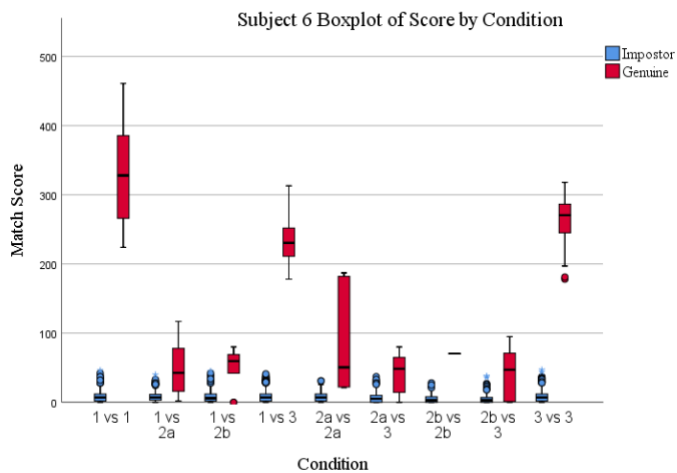
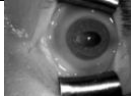
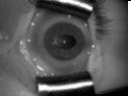
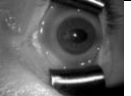
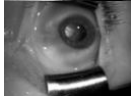
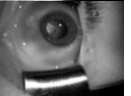
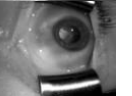
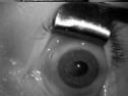
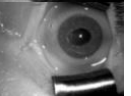
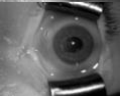
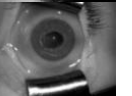
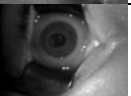
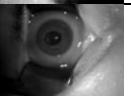
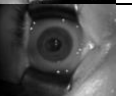
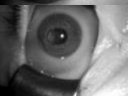
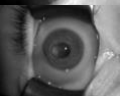
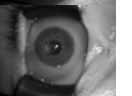
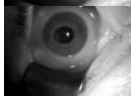
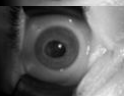
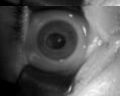
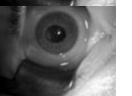


Figure 4.7: Subject 6 Match Score Boxplot by Condition

#### 4.1.7 Subject 7 Data Summary

Subject 7 was a 52-year-old female. Her cause of death was an overdose. There was no indication of what substance the individual used. The left pupil was slightly elongated and was not a circular shape. The subject also had minor decomposition visible on the surface of the skin. Table 4.11 shows the images captured of subject 7. The images of the left eye of subject 7 captured during condition 2 were placed into group 2b as they showed obvious signs of deflation. The images of the right eye of subject 7 captured during condition 2 were placed into group 2a as they did not show signs of obvious deflation.

Table 4.11: Subject 7 Image

| Eye and Condition | Capture Number  |   |   |   |   |
|-------------------|---|---|---|---|---|
|                   | 1   | 2   | 3   | 4   | 5   |
| LE 1              |    |    |    |    |    |
| LE 2              |   |   |   |   |   |
| LE 3              |  |  |  |  |  |
| RE 1              |  |  |  |  |  |
| RE 2              |  |  |  |  |  |
| RE 3              |  |  |  |  |  |

The subject 7 match score boxplot in Figure 4.8 shows that matching condition 2a to 2a and matching condition 3 to 3 provided high average genuine match scores. The lower genuine match scores for subject 7 are seen in the figure when matching conditions 1 vs 2b and 2b vs 3.

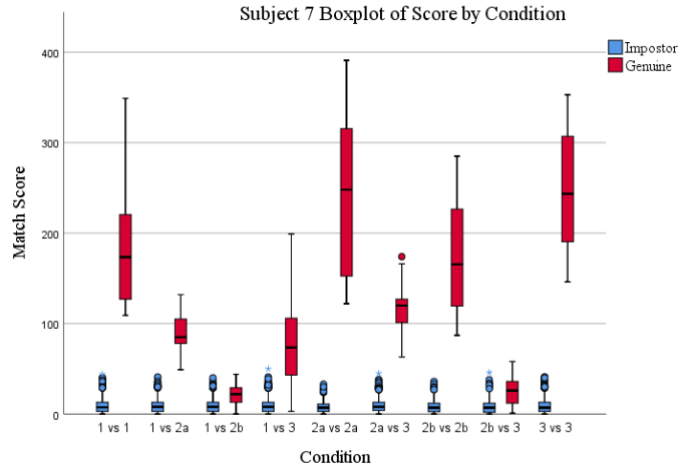


Figure 4.8: Subject 7 Match Score Boxplot by Condition

#### 4.1.8 Subject 8 Data Summary

Subject 8 was a 50-year-old male. His cause of death was an overdose. There was no indication of what substance the individual used. Table 4.12 shows the images captured of subject 8. The images of the left eye of subject 8 from condition 2 were placed into group 2b as they showed obvious signs of deflation. The images of the right eye of subject 8 from condition 2 were placed into group 2a as they did not show obvious signs of deflation.

Table 4.12: Subject 8 Images

| Eye and Condition | Capture Number |   |   |   |   |
|-------------------|----------------|---|---|---|---|
|                   | 1              | 2 | 3 | 4 | 5 |
| LE 1              |                |   |   |   |   |
| LE 2              |                |   |   |   |   |
| LE 3              |                |   |   |   |   |
| RE 1              |                |   |   |   |   |
| RE 2              |                |   |   |   |   |
| RE 3              |                |   |   |   |   |

The subject 8 match score boxplot in Figure 4.9 shows that matching condition 1 vs 1 provided the highest average genuine match score. The lower genuine match scores for subject 8 occurred when matching conditions 1 vs 2b, 2a vs 3, and 2b vs 3.

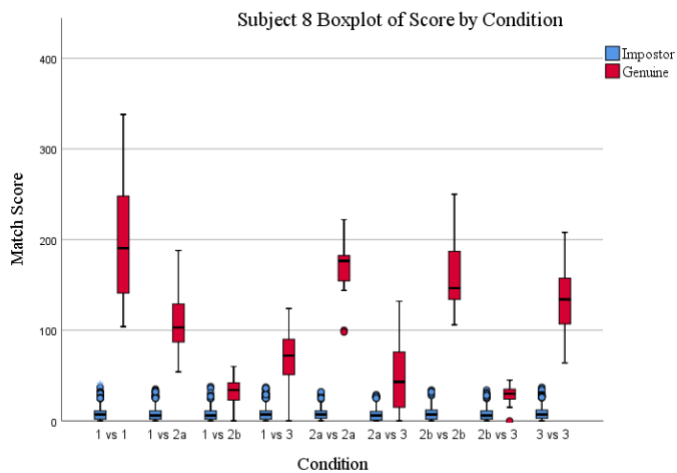
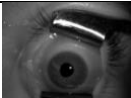
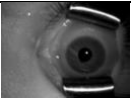
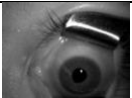
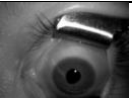
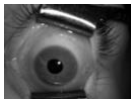
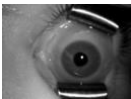
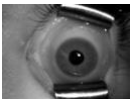
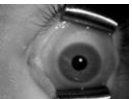
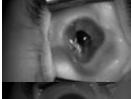
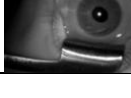


Figure 4.9: Subject 8 Match Score Boxplot by Condition

#### 4.1.9 Subject 9 Data Summary

Subject 9 was a 51-year-old female. Her cause of death was an overdose. There was no indication of what substance the individual used. Table 4.13 shows the images captured of subject 9. The right eye captures of subject 9 from condition 2 were placed into group 2b as they showed obvious signs of deflation. All five attempts of the left eye at condition 2 were unable to capture for subject 9. The attempts that failed to acquire are indicated by “FTA” in Table 4.13. The FTA’s could be a result of the deformation of the eye when the vitreous was removed.

Table 4.13: Subject 9 Images

| Eye and Condition | Capture Number  |   |   |  |   |
|-------------------|---|---|---|--|---|
|                   | 1   | 2   | 3   | 4  | 5   |
| LE 1              |    |    |    |    |    |
| LE 2              | FTA   | FTA   | FTA   | FTA  | FTA   |
| LE 3              |   |   |   |   |   |
| RE 1              |  |  |  |  |  |
| RE 2              |  |  |  |  |  |
| RE 3              |  |  |  |  |  |

The subject 9 match score boxplot in Figure 4.10 shows that matching condition 2b to condition 2b resulted in the highest average genuine match score. The matching of condition 1 to 2b and condition 2b to 3 both had low genuine match scores.

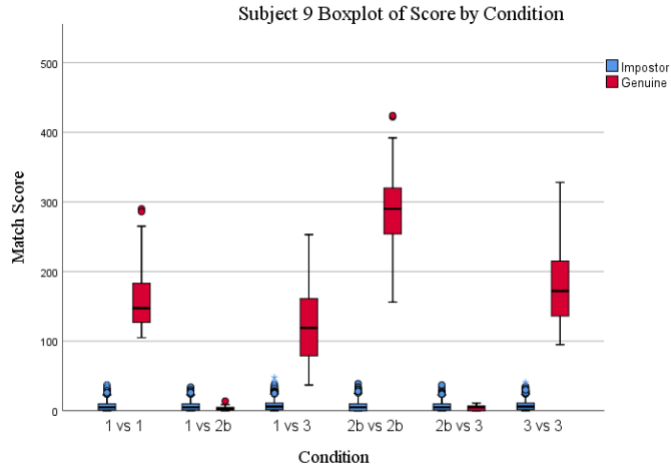


Figure 4.10: Subject 9 Match Score Boxplot by Condition

#### 4.1.10 Subject 10 Data Summary

Subject 10 was a 39-year-old female. Her cause of death was an overdose. There was no indication of what substance the individual used. Table 4.14 shows the images captured of subject 10. All of the images of subject 10 from condition 2 were placed into group 2b as they showed obvious signs of deflation.

Table 4.14: Subject 10 Images

| Eye and Condition | Capture Number |   |   |   |   |
|-------------------|----------------|---|---|---|---|
|                   | 1              | 2 | 3 | 4 | 5 |
| LE 1              |                |   |   |   |   |
| LE 2              |                |   |   |   |   |
| LE 3              |                |   |   |   |   |
| RE 1              |                |   |   |   |   |
| RE 2              |                |   |   |   |   |
| RE 3              |                |   |   |   |   |

The subject 10 match score boxplot in Figure 4.11 shows that the highest average genuine match score occurred when matching condition 3 to condition 3. The lower genuine match scores were matches between conditions 1 and 2b and between conditions 2b and 3. None of the genuine matches for subject 10 had a score below 100.

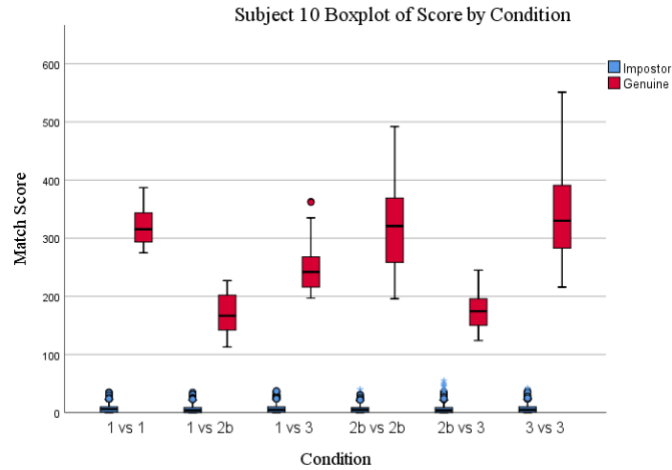


Figure 4.11: Subject 10 Match Score Boxplot by Condition

#### 4.1.11 Subject 11 Data Summary

Subject 11 was a 28-year-old male. His cause of death was an overdose. There was no indication of what substance the individual used. Table 4.15 shows the images captured of subject 11. All of the images of subject 11 from condition 2 were placed into group 2b as they showed obvious signs of deflation.

Table 4.15: Subject 11 Images

| Eye and Condition | Capture Number |   |   |   |   |
|-------------------|----------------|---|---|---|---|
|                   | 1              | 2 | 3 | 4 | 5 |
| LE 1              |                |   |   |   |   |
| LE 2              |                |   |   |   |   |
| LE 3              |                |   |   |   |   |
| RE 1              |                |   |   |   |   |
| RE 2              |                |   |   |   |   |
| RE 3              |                |   |   |   |   |

The subject 11 match score boxplot in Figure 4.12 shows that matching condition 1 vs condition 1 resulted in the highest average genuine score. The lowest genuine scores for subject 11 came from all of the matching involving condition 2b.

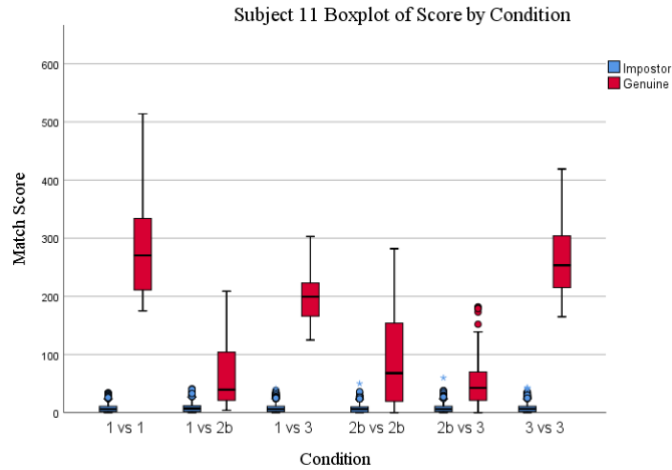
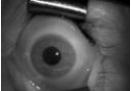
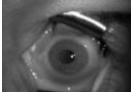
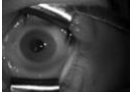
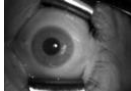
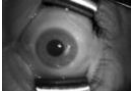
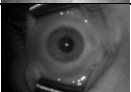
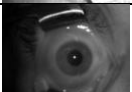
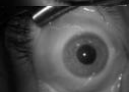


Figure 4.12: Subject 11 Match Score Boxplot by Condition

#### 4.1.12 Subject 12 Data Summary

Subject 12 was a 44-year-old male. His cause of death was determined to be natural, as there were no signs of drug use or foul play. Table 4.16 shows the images captured of subject 12. The left eye images from subject 12 captured during condition 2 were placed into group 2b as they showed obvious signs of deflation. The right eye images from subject 12 captured during condition 2 were placed into group 2a as they did not show obvious signs of deflation.

Table 4.16: Subject 12 Images

| Eye and Condition | Capture Number  |   |   |  |   |
|-------------------|---|---|---|--|---|
|                   | 1   | 2   | 3   | 4  | 5   |
| LE 1              |    |    |    |    |    |
| LE 2              |    |    |    |    |    |
| LE 3              |    |    |    |    |    |
| RE 1              |   |   |   |   |   |
| RE 2              |  |  |  |  |  |
| RE 3              |  |  |  |  |  |

The subject 12 match score boxplot in Figure 4.13 shows that matching condition 3 vs condition 3 resulted in the highest average genuine score. The lowest scores came from matching condition 2b vs condition 3, however none of the genuine score distributions overlap the imposter distributions for subject 12.

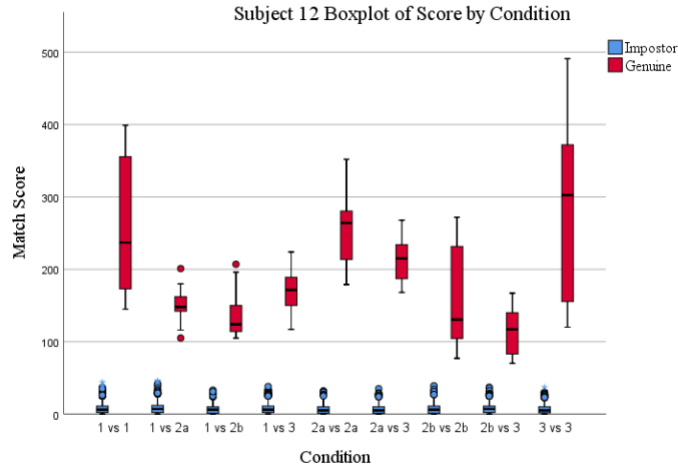
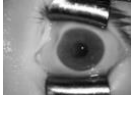
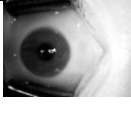


Figure 4.13: Subject 12 Match Score Boxplot by Condition

#### 4.1.13 Subject 13 Data Summary

Subject 13 was a 19-year-old male. His cause of death was determined to be related to a motor vehicle accident, the subject was on a bicycle and was struck by a car. The subject was in a coma for 10 days after the accident. There were no visible signs of trauma to the eyes of the subject at the time of the collection. Table 4.17 shows the images captured of subject 13. Only nine images were able to be captured from subject 13. The left eye captures of subject 13 from condition 2 were placed into group 2b as they showed obvious signs of deflation. The attempts that failed to acquire are indicated by “FTA” in Table 4.17. While the subject did not have any visible trauma to the head or eyes, he did experience a known loss of consciousness. Even in the case when trauma is not visible, it is possible for an individual to experience vision loss (Atkins, Newman, & Biousse, 2008). This may also have an effect on the ability of the IriShield device to capture an image.

Table 4.17: Subject 13 Images

| Eye and Condition | Capture Number  |   |   |     |     |
|-------------------|---|---|---|-----|-----|
|                   | 1   | 2   | 3   | 4   | 5   |
| LE 1              |  |  | FTA   | FTA | FTA |
| LE 2              |  |  |  | FTA | FTA |
| LE 3              |  | FTA   | FTA   | FTA | FTA |
| RE 1              |  |  |  | FTA | FTA |
| RE 2              | FTA   | FTA   | FTA   | FTA | FTA |
| RE 3              | FTA   | FTA   | FTA   | FTA | FTA |

The subject 13 match score boxplot in Figure 4.14 shows that the highest average genuine score for subject 13 occurred when matching condition 2b vs condition 2b. The lowest genuine match scores came from matching condition 1 vs condition 1, however that matching scenario also had the largest spread of scores.

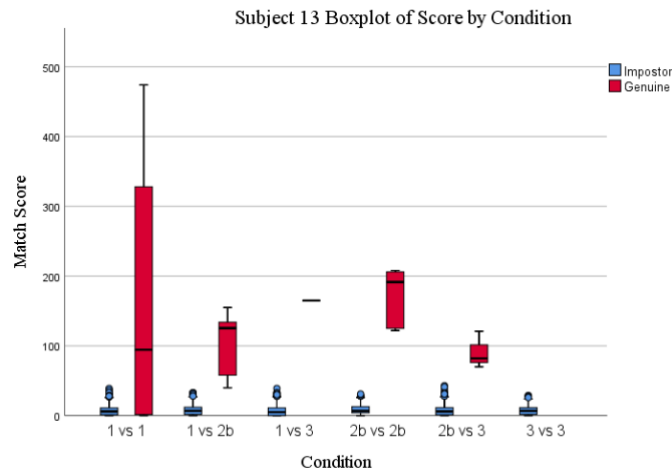
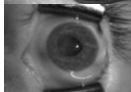
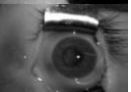
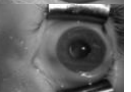
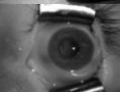
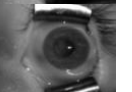
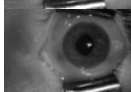
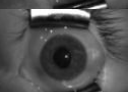
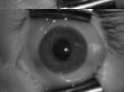


Figure 4.14: Subject 13 Match Score Boxplot by Condition

#### 4.1.14 Subject 14 Data Summary

Subject 14 was a 32-year-old male. His cause of death was an overdose. There was no indication of what substance the individual used. Table 4.18 shows the images captured of subject 14. The left eye images of subject 14 captured during condition 2 were placed into group 2b as they showed obvious signs of deflation. The right eye images of subject 14 captured during condition 2 were placed into group 2a as they did not show obvious signs of deflation.

Table 4.18: Subject 14 Images

| Eye and Condition | Capture Number  |   |   |   |   |
|-------------------|---|---|---|---|---|
|                   | 1   | 2   | 3   | 4   | 5   |
| LE 1              |    |    |    |    |    |
| LE 2              |    |    |    |    |    |
| LE 3              |    |    |    |    |    |
| RE 1              |   |   |   |   |   |
| RE 2              |  |  |  |  |  |
| RE 3              |  |  |  |  |  |

The subject 14 match score boxplot in Figure 4.15 shows that matching condition 1 to 1 provided the highest average genuine match score. Matching between conditions 2a and 2a, conditions 2b and 2b, and conditions 3 and 3 were also high for subject 14. The three worst matching scenarios were between conditions 1 and 2a, 1 and 2b, and 2b and 3.

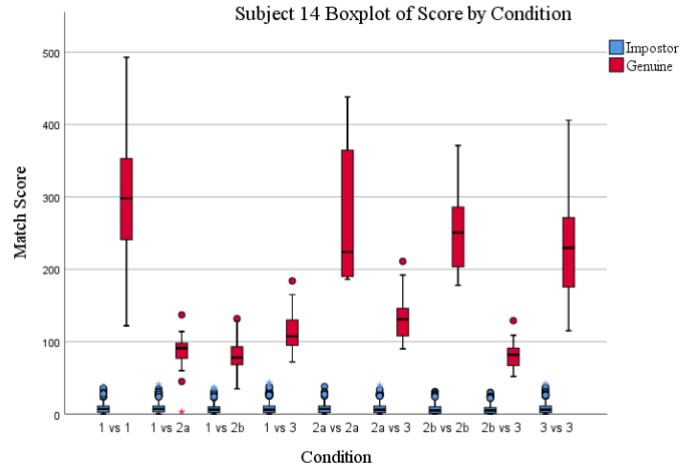


Figure 4.15: Subject 14 Match Score Boxplot by Condition

#### 4.1.15 Subject 15 Data Summary

Subject 15 was a 52-year-old male. His cause of death was determined to be natural, as there were no signs of drug use or foul play. Table 4.19 shows the images captured of subject 15. The left eye images of subject 15 captured during condition 2 were placed into group 2a as they did not show obvious signs of deflation. The right eye images of subject 15 captured during condition 2 were placed into group 2b as they showed obvious signs of deflation.

Table 4.19: Subject 15 Images

| Eye and Condition | Capture Number |   |   |   |   |
|-------------------|----------------|---|---|---|---|
|                   | 1              | 2 | 3 | 4 | 5 |
| LE 1              |                |   |   |   |   |
| LE 2              |                |   |   |   |   |
| LE 3              |                |   |   |   |   |
| RE 1              |                |   |   |   |   |
| RE 2              |                |   |   |   |   |
| RE 3              |                |   |   |   |   |

The subject 15 match score boxplot in Figure 4.16 shows that matching condition 3 to 3 provided the highest average genuine match score. Matching condition 2a vs 2a and 2b vs 2b provided genuine match scores that were also high. The lower genuine match scores for subject 15 occurred when matching conditions 1 vs 2b and 2b vs 3.

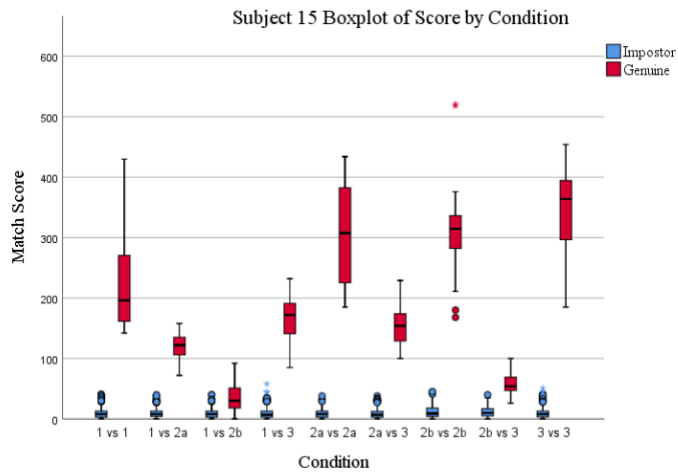


Figure 4.16: Subject 15 Match Score Boxplot by Condition

## 4.2 Analysis of Image Quality

The image quality statistics were determined using Neurotechnology SDK 10. The output of the image quality was analyzed using SPSS statistics. Quality is the overall quality score of the image. The other metrics, iris detection confidence, iris pupil concentricity, iris pupil contrast, iris radius, iris sclera contrast, margin adequacy, pupil boundary circularity, pupil to iris ratio, sharpness, and usable iris area are more descriptive metrics of the images. The analysis of the other quality metrics helps determine which metrics can be attributed to any change in quality.

Descriptive statistics of the quality score of each condition were found. The descriptive statistics for quality across the four conditions are shown in Table 4.20. Boxplots were created to show the distributions of image quality of each condition in Figure 4.17. Example images from each condition with the maximum, mean, and minimum image quality scores are shown in Table 4.21.

Table 4.20: Descriptive Statistics of Image Quality by Condition

| <b>Condition</b> | <b>N</b> | <b>Mean</b> | <b>Std. Deviation</b> | <b>Minimum</b> | <b>Maximum</b> |
|------------------|----------|-------------|-----------------------|----------------|----------------|
| <b>1</b>         | 145      | 81.55       | 11.137                | 48             | 100            |
| <b>2a</b>        | 54       | 78.41       | 8.504                 | 58             | 93             |
| <b>2b</b>        | 76       | 68.21       | 16.489                | 28             | 98             |
| <b>3</b>         | 141      | 82.38       | 7.594                 | 63             | 100            |

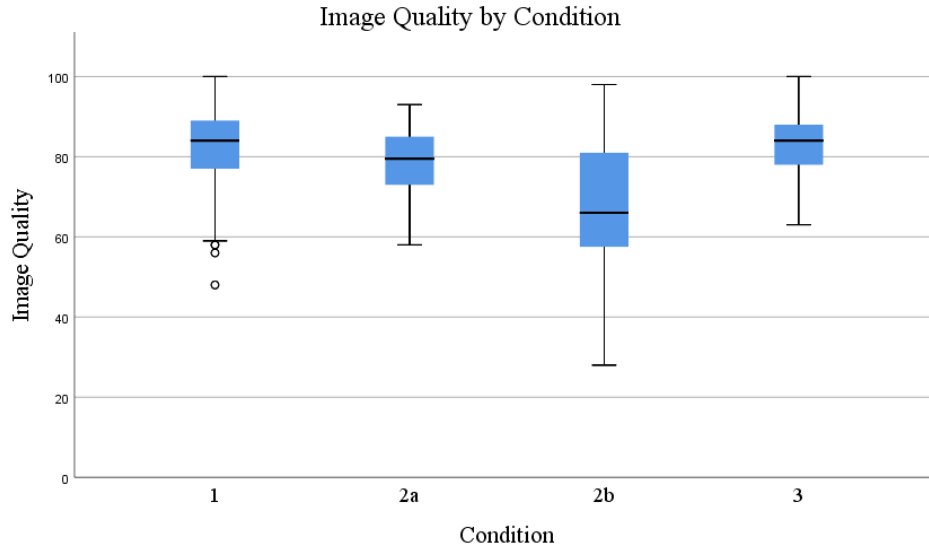


Figure 4.17: Boxplot of Image Quality by Condition

Table 4.21: Image Quality Examples by Condition

| Condition | Maximum | Mean | Minimum |
|-----------|---------|------|---------|
| 1         |         |      |         |
| 2a        |         |      |         |
| 2b        |         |      |         |
| 3         |         |      |         |

The average quality score for conditions 1, 2a, and 3 are 81.55, 78.41, and 82.38 respectively. The averages for conditions 1, 2a, and 3 are within the high-quality level. The average quality score for condition 2b is 68.21. This is in the medium quality level and is classified as an acceptable quality (JTC 1/SC 37, 2005).

The following analysis tests the hypothesis that the means of image quality for the four different conditions are all the same.

$$H_0: \mu_{Condition 1} = \mu_{Condition 2a} = \mu_{Condition 2b} = \mu_{Condition 3}$$

$$H_a: \text{Not all the means are equal}$$

The *Levene's F* test revealed that the homogeneity of variance assumption was not met ( $p < 0.001$ ). The *Welch's F* test was used. An alpha level of 0.05 was used for all subsequent analyses. The one-way ANOVA of condition on image quality revealed a statistically significant main effect, *Welch's F*(3, 163.395) = 18.264,  $p < 0.05$ . This indicated that not all conditions had the same mean quality score. The estimated omega squared (est.  $\omega^2 = 0.11$ ) indicated that approximately 11% of the total variation in quality score is attributable to the condition. This is a medium effect size.

Post hoc comparisons, using the Games-Howell post hoc procedure, were conducted to determine which pairs of the four conditions means differed significantly. These revealed that images captured during condition 2b had a significantly lower quality compared to images captured from condition 1 ( $p < 0.001$ ), condition 2a ( $p < 0.001$ ), and to condition 3 ( $p < 0.001$ ). Condition 2a also had significantly lower quality compared to images from condition 3 ( $p = 0.018$ ). There was no significant mean difference between any of the other conditions.

#### 4.2.1 Iris Detection Confidence Analysis

Descriptive statistics of the iris detection confidence of each condition were found. The descriptive statistics for iris detection confidence across the four conditions are shown in Table 4.22. Boxplots were created to show the distributions of iris detection confidence of each condition in Figure 4.18.

Table 4.22: Descriptive Statistics of Iris Detection Confidence by Condition

| Condition | N   | Mean  | Std. Deviation | Minimum | Maximum |
|-----------|-----|-------|----------------|---------|---------|
| <b>1</b>  | 145 | 79.51 | 19.467         | 11      | 97      |
| <b>2a</b> | 54  | 80.76 | 18.896         | 17      | 95      |
| <b>2b</b> | 76  | 65.57 | 19.812         | 17      | 95      |
| <b>3</b>  | 141 | 84.94 | 15.395         | 15      | 97      |

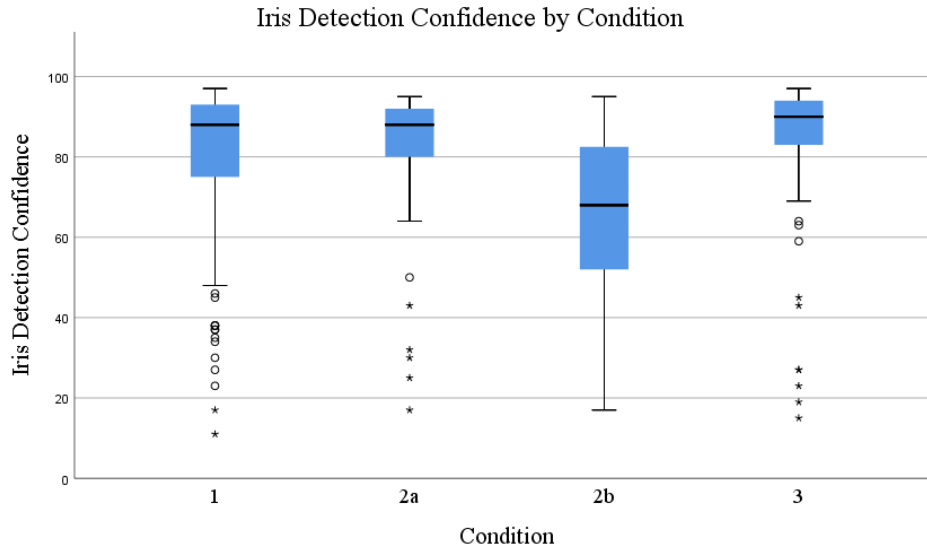


Figure 4.18: Boxplot of Iris Detection Confidence by Condition

The following analysis tests the hypothesis that the means of iris detection confidence for the four different conditions are all the same.

$$H_0: \mu_{Condition 1} = \mu_{Condition 2a} = \mu_{Condition 2b} = \mu_{Condition 3}$$

$$H_a: \text{Not all the means are equal}$$

The *Levene's F* test revealed that the homogeneity of variance assumption was not met ( $p < 0.001$ ). The *Welch's F* test was used. An alpha level of 0.05 was used for all subsequent analyses. The one-way ANOVA of condition on iris detection confidence revealed a statistically significant main effect, *Welch's F*(3, 165.658) = 18.204,  $p < 0.05$ . This indicated that not all conditions had the same mean iris detection confidence score. The estimated omega squared (est.

$\omega^2 = 0.11$ ) indicated that approximately 11% of the total variation in iris detection confidence is attributable to the condition. This is a medium effect size.

Post hoc comparisons, using the Games-Howell post hoc procedure, were conducted to determine which pairs of the four conditions means differed significantly. These revealed that images captured during condition 2b had a significantly lower iris detection confidence compared to images captured from condition 1 ( $p < 0.001$ ), condition 2a ( $p < 0.001$ ), and condition 3 ( $p < 0.001$ ). There was no significant mean difference between any of the other conditions.

#### 4.2.2 Iris Pupil Concentricity Analysis

Descriptive statistics of the iris pupil concentricity of each condition were found. The descriptive statistics for iris pupil concentricity across the four conditions are shown in Table 4.23. Boxplots were created to show the distributions of iris pupil concentricity of each condition in Figure 4.19.

Table 4.23: Descriptive Statistics of Iris Pupil Concentricity by Condition

| <b>Condition</b> | <b>N</b> | <b>Mean</b> | <b>Std. Deviation</b> | <b>Minimum</b> | <b>Maximum</b> |
|------------------|----------|-------------|-----------------------|----------------|----------------|
| <b>1</b>         | 145      | 97.47       | 1.225                 | 93             | 100            |
| <b>2a</b>        | 54       | 97.67       | 1.009                 | 95             | 100            |
| <b>2b</b>        | 76       | 97.42       | 1.635                 | 92             | 100            |
| <b>3</b>         | 141      | 97.60       | 0.985                 | 96             | 100            |

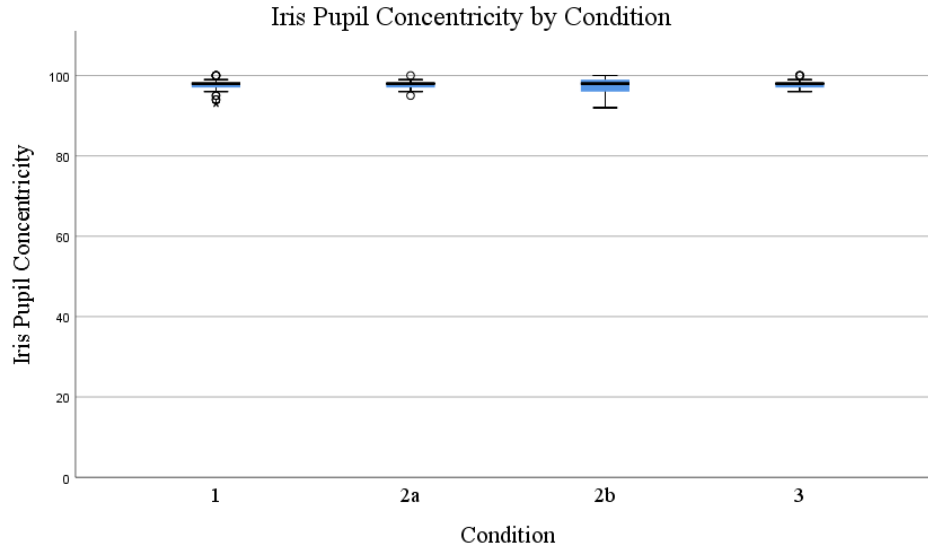


Figure 4.19: Boxplot of Iris Pupil Concentricity by Condition

The following analysis tests the hypothesis that the means of iris pupil concentricity for the four different conditions are all the same.

$$H_0: \mu_{Condition 1} = \mu_{Condition 2a} = \mu_{Condition 2b} = \mu_{Condition 3}$$

$$H_a: \text{Not all the means are equal}$$

The *Levene's F* test revealed that the homogeneity of variance assumption was not met ( $p < 0.001$ ). The *Welch's F* test was used. An alpha level of 0.05 was used for all subsequent analyses. The one-way ANOVA of condition on iris pupil concentricity revealed that there was not a statistically significant main effect, *Welch's F*(3, 167.428) = 0.733,  $p > 0.05$ . This indicated that all of the means of iris pupil concentricity were the same. The estimated omega squared (est.  $\omega^2 = 0.001$ ) indicated that approximately 0.1% of the total variation in iris pupil concentricity is attributable to the condition. This is a very small effect size.

#### 4.2.3 Iris Pupil Contrast Analysis

Descriptive statistics of the iris pupil contrast of each condition were found. The descriptive statistics for iris pupil contrast across the four conditions are shown in Table 4.24.

Boxplots were created to show the distributions of iris pupil contrast of each condition in Figure 4.20.

Table 4.24: Descriptive Statistics of Iris Pupil Contrast by Condition

| Condition | N   | Mean  | Std. Deviation | Minimum | Maximum |
|-----------|-----|-------|----------------|---------|---------|
| <b>1</b>  | 145 | 49.88 | 16.269         | 5       | 75      |
| <b>2a</b> | 54  | 48.57 | 11.982         | 16      | 67      |
| <b>2b</b> | 76  | 40.53 | 18.986         | 3       | 68      |
| <b>3</b>  | 141 | 52.05 | 14.527         | 9       | 77      |

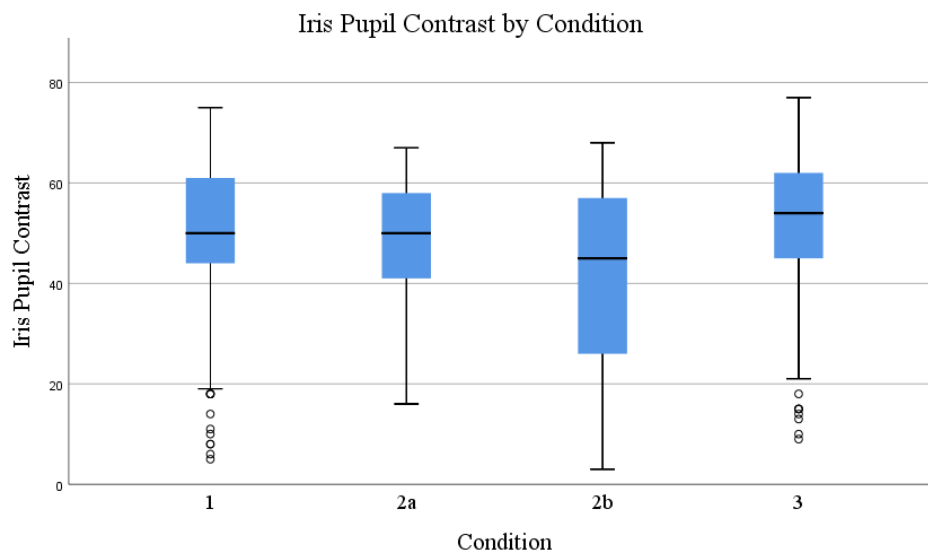


Figure 4.20: Boxplot of Iris Pupil Contrast by Condition

The following analysis tests the hypothesis that the means of iris pupil contrast for the four different conditions are all the same.

$$H_0: \mu_{Condition\ 1} = \mu_{Condition\ 2a} = \mu_{Condition\ 2b} = \mu_{Condition\ 3}$$

$$H_a: \text{Not all the means are equal}$$

The *Levene's F* test revealed that the homogeneity of variance assumption was not met ( $p < 0.001$ ). The *Welch's F* test was used. An alpha level of 0.05 was used for all subsequent analyses. The one-way ANOVA of condition on iris pupil contrast revealed a statistically

significant main effect, *Welch's*  $F(3, 176.00) = 7.167, p < 0.05$ . This indicated that not all conditions had the same mean iris pupil contrast score. The estimated omega squared (est.  $\omega^2 = 0.04$ ) indicated that approximately 4% of the total variation in iris pupil contrast is attributable to the condition. This is a small effect size.

Post hoc comparisons, using the Games-Howell post hoc procedure, were conducted to determine which pairs of the four conditions means differed significantly. These revealed that images captured during condition 2b had a significantly lower iris pupil contrast compared to images captured from condition 1 ( $p = 0.002$ ), condition 2a ( $p = 0.019$ ), and condition 3 ( $p < 0.001$ ). There was no significant mean difference between any of the other conditions.

#### 4.2.4 Iris Radius Analysis

Descriptive statistics of the iris radius of each condition were found. The descriptive statistics for iris radius across the four conditions are shown in Table 4.25. Boxplots were created to show the distributions of iris radius of each condition in Figure 4.21.

Table 4.25: Descriptive Statistics of Iris Radius by Condition

| <b>Condition</b> | <b>N</b> | <b>Mean</b> | <b>Std. Deviation</b> | <b>Minimum</b> | <b>Maximum</b> |
|------------------|----------|-------------|-----------------------|----------------|----------------|
| <b>1</b>         | 145      | 103.90      | 1.001                 | 88             | 195            |
| <b>2a</b>        | 54       | 103.76      | 1.353                 | 86             | 128            |
| <b>2b</b>        | 76       | 99.04       | 1.243                 | 78             | 123            |
| <b>3</b>         | 141      | 103.10      | 0.737                 | 85             | 128            |

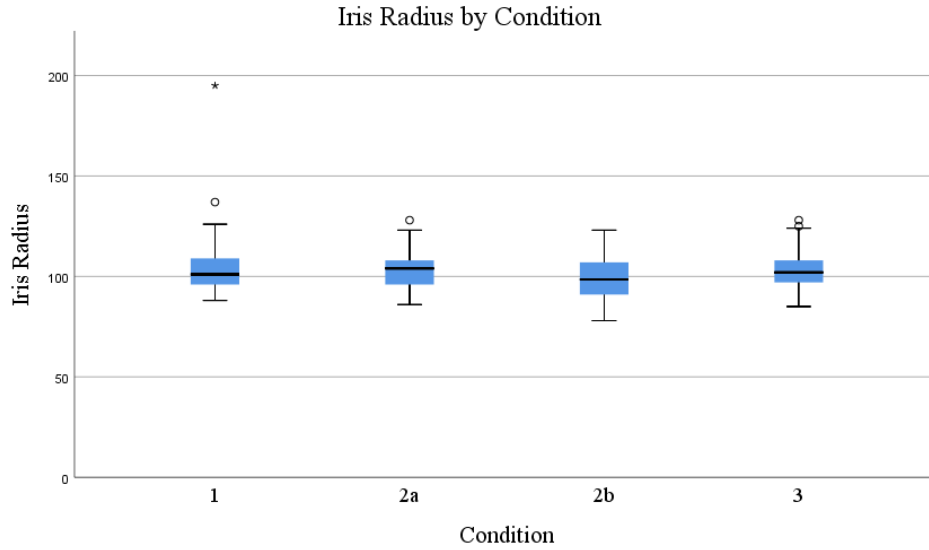


Figure 4.21: Boxplot of Iris Radius by Condition

The following analysis tests the hypothesis that the means of iris radius for the four different conditions are all the same.

$$H_0: \mu_{Condition 1} = \mu_{Condition 2a} = \mu_{Condition 2b} = \mu_{Condition 3}$$

$$H_a: \text{Not all the means are equal}$$

The *Levene's F* test revealed that the homogeneity of variance assumption was met ( $p < 0.188$ ). The *Welch's F* test was used. An alpha level of 0.05 was used for all subsequent analyses. The one-way ANOVA of condition on iris radius revealed a statistically significant main effect, *Welch's F*(3, 169.264) = 3.639,  $p < 0.05$ . This indicated that not all conditions had the same mean iris radius value. The estimated omega squared (est.  $\omega^2 = 0.018$ ) indicated that approximately 2% of the total variation in iris radius is attributable to the condition. This is a small effect size.

Post hoc comparisons, using the Games-Howell post hoc procedure, were conducted to determine which pairs of the four conditions means differed significantly. These revealed that images captured during condition 2b had a significantly lower iris detection confidence compared to images captured from condition 1 ( $p = 0.014$ ) and condition 3 ( $p < 0.029$ ). There was no significant mean difference between any of the other conditions.

### 4.2.5 Iris Sclera Contrast Analysis

Descriptive statistics of the iris sclera contrast of each condition were found. The descriptive statistics for iris sclera contrast across the four conditions are shown in Table 4.26. Boxplots were created to show the distributions of iris sclera contrast of each condition in Figure 4.22.

Table 4.26: Descriptive Statistics of Iris Sclera Contrast by Condition

| Condition | N   | Mean  | Std. Deviation | Minimum | Maximum |
|-----------|-----|-------|----------------|---------|---------|
| <b>1</b>  | 145 | 29.28 | 8.099          | 5       | 54      |
| <b>2a</b> | 54  | 28.50 | 7.011          | 14      | 44      |
| <b>2b</b> | 76  | 27.01 | 8.206          | 14      | 47      |
| <b>3</b>  | 141 | 29.41 | 7.039          | 10      | 49      |

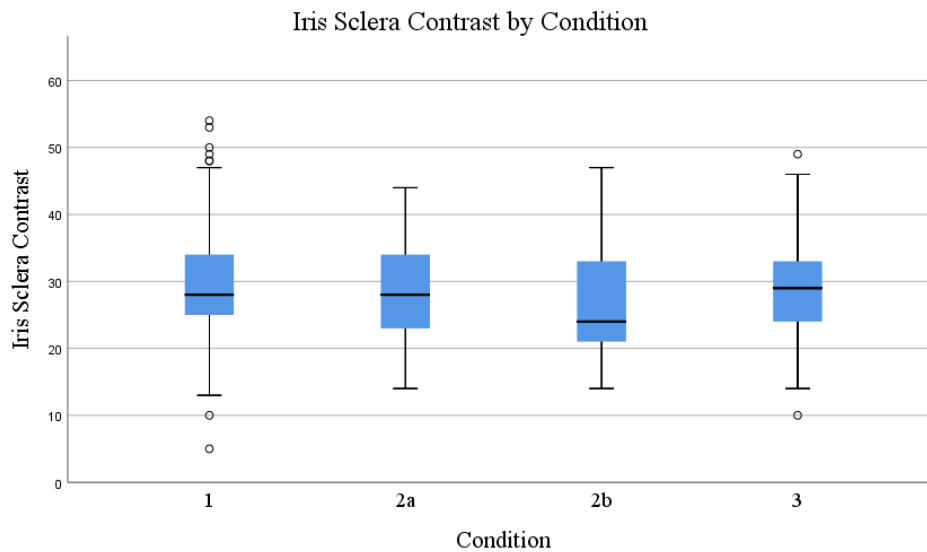


Figure 4.22: Boxplot of Iris Sclera Contrast by Condition

The following analysis tests the hypothesis that the means of iris sclera contrast for the four different conditions are all the same.

$$H_0: \mu_{Condition 1} = \mu_{Condition 2a} = \mu_{Condition 2b} = \mu_{Condition 3}$$

$$H_a: \text{Not all the means are equal}$$

The *Levene's F* test revealed that the homogeneity of variance assumption was met ( $p = 0.291$ ). The *Welch's F* test was used. An alpha level of 0.05 was used for all subsequent analyses. The one-way ANOVA of condition on iris sclera contrast revealed that there was not a statistically significant main effect,  $Welch's F(3, 171.539) = 1.737, p > 0.05$ . This indicated that all conditions had the same mean iris sclera contrast score. The estimated omega squared (est.  $\omega^2 = 0.005$ ) indicated that approximately 0.5% of the total variation in iris sclera contrast is attributable to the condition. This is a very small effect size.

#### 4.2.6 Margin Adequacy Analysis

Descriptive statistics of the margin adequacy of each condition were found. The descriptive statistics for margin adequacy across the four conditions are shown in Table 4.27. Boxplots were created to show the distributions of margin adequacy of each condition in Figure 4.23.

Table 4.27: Descriptive Statistics of Margin Adequacy by Condition

| <b>Condition</b> | <b>N</b> | <b>Mean</b> | <b>Std. Deviation</b> | <b>Minimum</b> | <b>Maximum</b> |
|------------------|----------|-------------|-----------------------|----------------|----------------|
| <b>1</b>         | 145      | 93.14       | 19.361                | 5              | 100            |
| <b>2a</b>        | 54       | 93.20       | 18.338                | 4              | 100            |
| <b>2b</b>        | 76       | 97.43       | 12.523                | 24             | 100            |
| <b>3</b>         | 141      | 95.69       | 14.319                | 22             | 100            |

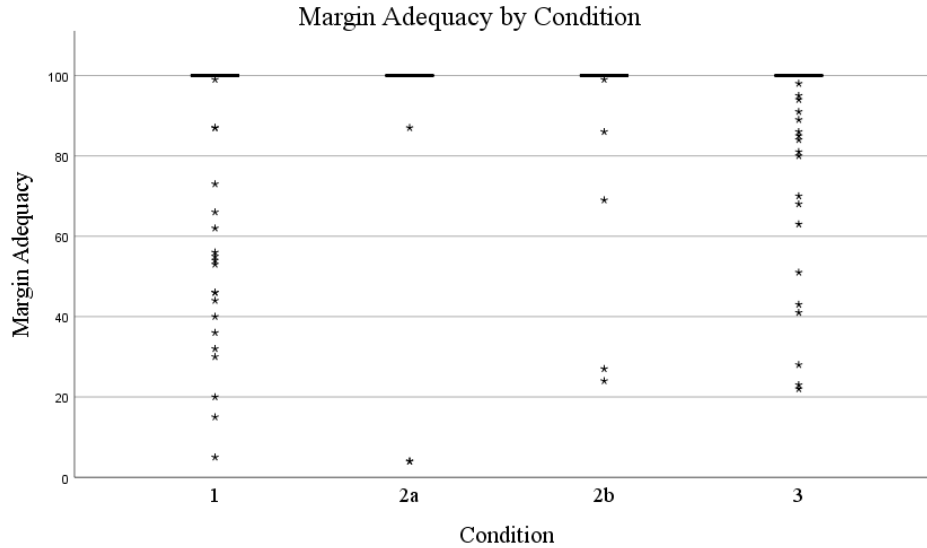


Figure 4.23: Boxplot of Margin Adequacy by Condition

The following analysis tests the hypothesis that the means of margin adequacy for the four different conditions are all the same.

$$H_0: \mu_{Condition\ 1} = \mu_{Condition\ 2a} = \mu_{Condition\ 2b} = \mu_{Condition\ 3}$$

$$H_a: \text{Not all the means are equal}$$

The *Levene's F* test revealed that the homogeneity of variance assumption was not met ( $p = 0.002$ ). The *Welch's F* test was used. An alpha level of 0.05 was used for all subsequent analyses. The one-way ANOVA of condition on margin adequacy revealed a statistically significant main effect, *Welch's F*(3, 171.642) = 1.330,  $p > 0.05$ . This indicated that all conditions had the same mean margin adequacy score. The estimated omega squared (est.  $\omega^2 = 0.002$ ) indicated that approximately 0.2% of the total variation in margin adequacy is attributable to the condition. This is a very small effect size.

### 4.2.7 Pupil Boundary Circularity Analysis

Descriptive statistics of the pupil boundary circularity of each condition were found. The descriptive statistics for pupil boundary circularity across the four conditions are shown in Table 4.28. Boxplots were created to show the distributions of pupil boundary circularity of each condition in Figure 4.24.

Table 4.28: Descriptive Statistics of Pupil Boundary Circularity by Condition

| Condition | N   | Mean  | Std. Deviation | Minimum | Maximum |
|-----------|-----|-------|----------------|---------|---------|
| <b>1</b>  | 145 | 89.09 | 19.139         | 9       | 100     |
| <b>2a</b> | 54  | 68.63 | 23.402         | 12      | 95      |
| <b>2b</b> | 76  | 63.26 | 30.264         | 1       | 98      |
| <b>3</b>  | 141 | 86.60 | 16.256         | 33      | 99      |

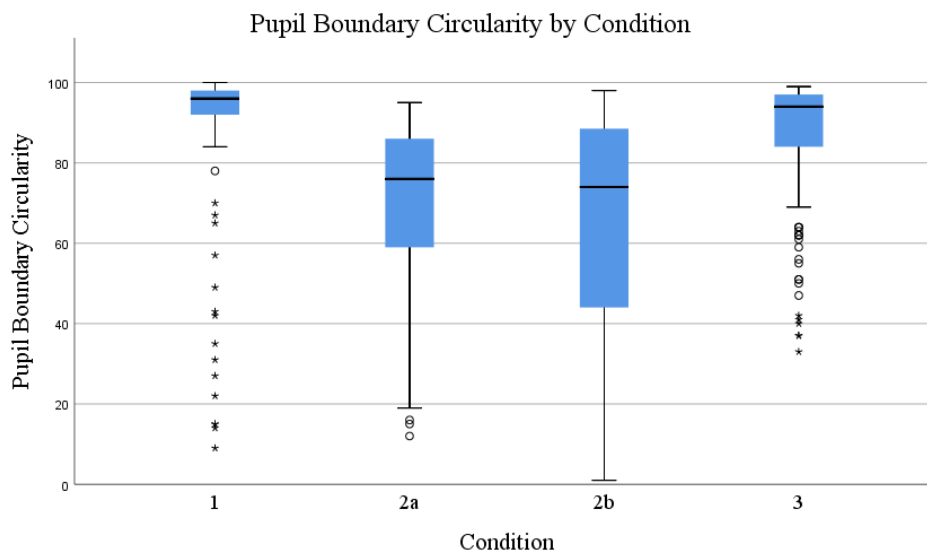


Figure 4.24: Boxplot of Pupil Boundary Circularity by Condition

The following analysis tests the hypothesis that the means of pupil boundary circularity for the four different conditions are all the same.

$$H_0: \mu_{Condition\ 1} = \mu_{Condition\ 2a} = \mu_{Condition\ 2b} = \mu_{Condition\ 3}$$

$$H_a: \text{Not all the means are equal}$$

The *Levene's F* test revealed that the homogeneity of variance assumption was not met ( $p < 0.001$ ). The *Welch's F* test was used. An alpha level of 0.05 was used for all subsequent analyses. The one-way ANOVA of condition on pupil boundary circularity revealed a statistically significant main effect, *Welch's F*(3, 156.788) = 24.063,  $p < 0.05$ . This indicated that not all conditions had the same mean pupil boundary circularity. The estimated omega squared (est.  $\omega^2 = 0.14$ ) indicated that approximately 14% of the total variation in pupil boundary circularity is attributable to the condition. This is a large effect size.

Post hoc comparisons, using the Games-Howell post hoc procedure, were conducted to determine which pairs of the four conditions means differed significantly. These revealed that images captured during condition 2a had a significantly lower pupil boundary circularity compared to images captured from condition 1 ( $p < 0.001$ ) and condition 3 ( $p < 0.001$ ). It also revealed that images captured during condition 2b had a significantly lower pupil boundary circularity compared to images captured from condition 1 ( $p < 0.001$ ) and condition 3 ( $p < 0.001$ ). There was no significant mean difference between any of the other conditions.

#### 4.2.8 Pupil to Iris Ratio Analysis

Descriptive statistics of the pupil to iris ratio of each condition were found. The descriptive statistics for pupil to iris ratio across the four conditions are shown in Table 4.29. Boxplots were created to show the distributions of pupil to iris ratio of each condition in Figure 4.25.

Table 4.29: Descriptive Statistics of Pupil to Iris Ratio by Condition

| <b>Condition</b> | <b>N</b> | <b>Mean</b> | <b>Std. Deviation</b> | <b>Minimum</b> | <b>Maximum</b> |
|------------------|----------|-------------|-----------------------|----------------|----------------|
| <b>1</b>         | 145      | 43.19       | 4.566                 | 35             | 56             |
| <b>2a</b>        | 54       | 42.35       | 3.405                 | 36             | 58             |
| <b>2b</b>        | 76       | 42.07       | 4.717                 | 34             | 55             |
| <b>3</b>         | 141      | 42.31       | 3.840                 | 35             | 55             |

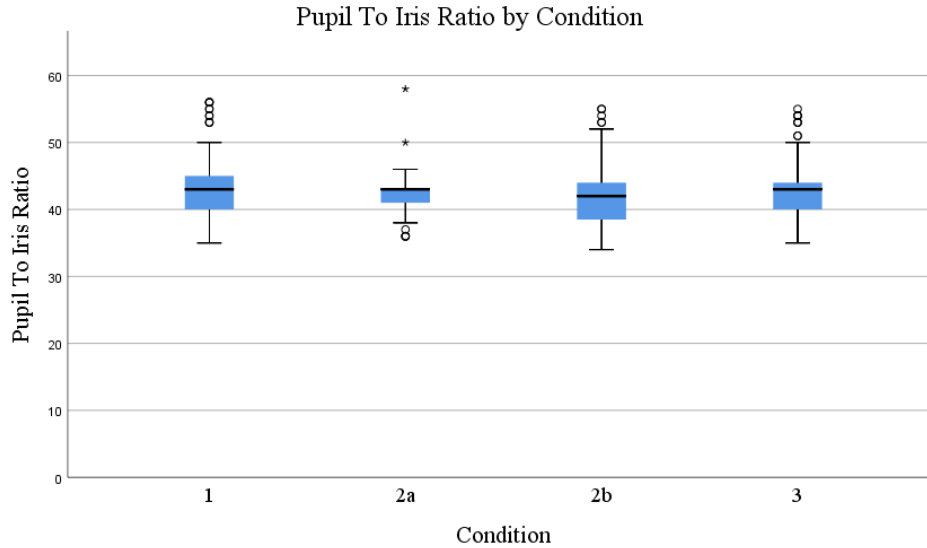


Figure 4.25: Boxplot of Pupil to Iris Ratio by Condition

The following analysis tests the hypothesis that the means of pupil to iris ratio for the four different conditions are all the same.

$$H_0: \mu_{\text{Condition 1}} = \mu_{\text{Condition 2a}} = \mu_{\text{Condition 2b}} = \mu_{\text{Condition 3}}$$

$$H_a: \text{Not all the means are equal}$$

The *Levene's F* test revealed that the homogeneity of variance assumption was not met ( $p = 0.008$ ). The *Welch's F* test was used. An alpha level of 0.05 was used for all subsequent analyses. The one-way ANOVA of condition on pupil to iris ratio revealed that there was not a statistically significant main effect, *Welch's F* ( $F(3, 175.30) = 1.454, p > 0.05$ ). This indicated that all conditions had the same mean pupil to iris ratio. The estimated omega squared (est.  $\omega^2 = 0.003$ ) indicated that approximately 0.3% of the total variation in pupil to iris ratio is attributable to the condition. This is a very small effect size.

### 4.2.9 Sharpness Analysis

Descriptive statistics of the sharpness of each condition were found. The descriptive statistics for sharpness across the four conditions are shown in Table 4.30. Boxplots were created to show the distributions of sharpness of each condition in Figure 4.26.

Table 4.30: Descriptive Statistics of Sharpness by Condition

| Condition | N   | Mean  | Std. Deviation | Minimum | Maximum |
|-----------|-----|-------|----------------|---------|---------|
| <b>1</b>  | 145 | 19.30 | 9.758          | 2       | 51      |
| <b>2a</b> | 54  | 19.33 | 8.626          | 7       | 49      |
| <b>2b</b> | 76  | 21.08 | 9.740          | 6       | 46      |
| <b>3</b>  | 141 | 18.57 | 10.032         | 1       | 50      |

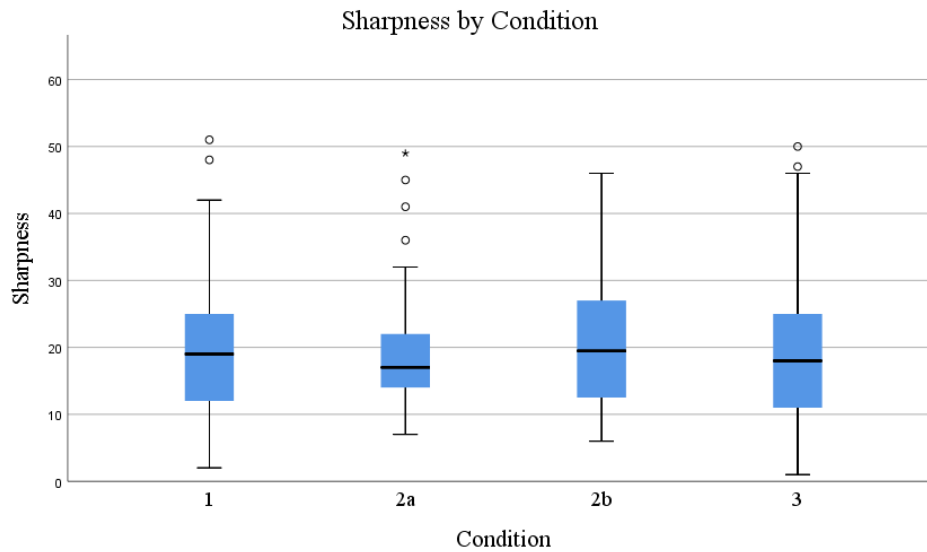


Figure 4.26: Boxplot of Sharpness by Condition

The following analysis tests the hypothesis that the means of sharpness for the four different conditions are all the same.

$$H_0: \mu_{\text{Condition 1}} = \mu_{\text{Condition 2a}} = \mu_{\text{Condition 2b}} = \mu_{\text{Condition 3}}$$

$$H_a: \text{Not all the means are equal}$$

The *Levene's F* test revealed that the homogeneity of variance assumption was met ( $p = 0.232$ ). The *Welch's F* test was used. An alpha level of 0.05 was used for all subsequent

analyses. The one-way ANOVA of condition on sharpness revealed that there was not a statistically significant main effect, *Welch's*  $F(3, 175.186) = 1.069, p > 0.05$ . This indicated that all conditions had the same mean sharpness score. The estimated omega squared (est.  $\omega^2 = 0.0004$ ) indicated that approximately 0% of the total variation in sharpness is attributable to the condition. This is a very small effect size.

#### 4.2.10 Usable Iris Area Analysis

Descriptive statistics of the usable iris area of each condition were found. The descriptive statistics for usable iris area across the four conditions are shown in Table 4.31. Boxplots were created to show the distributions of usable iris area of each condition in Figure 4.27.

Table 4.31: Descriptive Statistics of Usable Iris Area by Condition

| Condition | N   | Mean  | Std. Deviation | Minimum | Maximum |
|-----------|-----|-------|----------------|---------|---------|
| <b>1</b>  | 145 | 99.26 | 3.021          | 71      | 100     |
| <b>2a</b> | 54  | 99.65 | .828           | 96      | 100     |
| <b>2b</b> | 76  | 96.41 | 6.680          | 62      | 100     |
| <b>3</b>  | 141 | 99.68 | 1.541          | 86      | 100     |

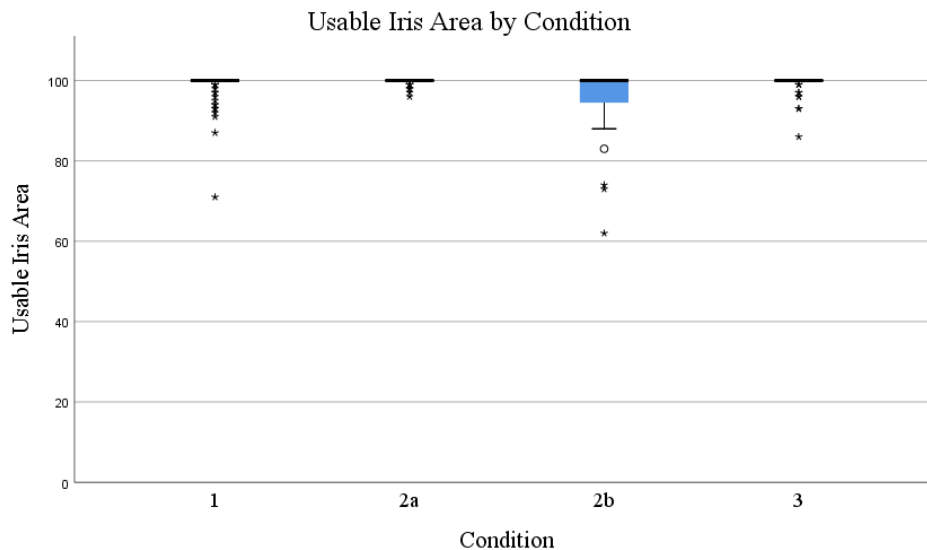


Figure 4.27: Boxplot of Usable Iris Area by Condition

The following analysis tests the hypothesis that the means of usable iris area for the four different conditions are all the same.

$$H_0: \mu_{Condition 1} = \mu_{Condition 2a} = \mu_{Condition 2b} = \mu_{Condition 3}$$

$$H_a: \text{Not all the means are equal}$$

The *Levene's F* test revealed that the homogeneity of variance assumption was not met ( $p < 0.001$ ). The *Welch's F* test was used. An alpha level of 0.05 was used for all subsequent analyses. The one-way ANOVA of condition on usable iris area revealed a statistically significant main effect, *Welch's F*(3, 192.427) = 6.525,  $p < 0.05$ . This indicated that not all conditions had the same mean usable iris area score. The estimated omega squared (est.  $\omega^2 = 0.038$ ) indicated that approximately 4% of the total variation in usable iris area is attributable to the condition. This is a small effect size.

Post hoc comparisons, using the Games-Howell post hoc procedure, were conducted to determine which pairs of the four conditions means differed significantly. These revealed that images captured during condition 2b had a significantly lower usable iris area compared to images captured from condition 1 ( $p = 0.003$ ), condition 2a ( $p < 0.001$ ), and condition 3 ( $p < 0.001$ ). There was no significant mean difference between any of the other conditions.

In summary, the image quality analysis showed that there were significant differences among the conditions for many of the metrics. The average image quality score for condition 2a was significantly lower than that of the other conditions. Image quality of condition 2a was significantly lower than that of conditions 1 and 3. Among the other metrics, condition 2b was significantly lower than the other conditions for the iris detection confidence, the iris-pupil contrast, the iris radius, the pupil boundary circularity, and the usable iris area. Condition 2a was lower than conditions 1 and 3 for the pupil boundary circularity. The pupil concentricity, iris-sclera contrast, margin adequacy, pupil to iris ratio, and sharpness showed no statistical difference between the conditions. Interestingly, conditions 1 and 3 were not statistically different for any of the image quality metrics.

### 4.3 Analysis of Matching Performance

Matching was performed across conditions, using one condition for the enrollment images and another for the verification images. The possible combinations were chosen only using a condition as the verification condition if it occurred at the same time as the enrollment or afterwards. Matching performance was measured using DET curves. The DET curves show the equal error rate (EER) for each matching scenario as well as the false reject rate (FRR) at three pre-selected false accept rates (FAR). The matching performance summary is shown in Table 4.32.

Table 4.32: Matching Performance Summary

| Enrollment Condition | Verification Condition | EER    | FRR      |            |             |
|----------------------|------------------------|--------|----------|------------|-------------|
|                      |                        |        | FAR = 1% | FAR = 0.1% | FAR = 0.01% |
| 1                    | 1                      | 3.93%  | 4.23%    | 4.75%      | 4.93%       |
| 1                    | 2a                     | 10.49% | 12.96%   | 14.66%     | 16.85%      |
| 1                    | 2b                     | 24.96% | 42.43%   | 48.88%     | 52.00%      |
| 1                    | 3                      | 3.15%  | 4.17%    | 5.80%      | 8.98%       |
| 2a                   | 2a                     | 0.90%  | 0.97%    | 0.97%      | 0.97%       |
| 2a                   | 3                      | 5.25%  | 7.04%    | 8.23%      | 11.35%      |
| 2b                   | 2b                     | 9.25%  | 12.50%   | 13.82%     | 15.25%      |
| 2b                   | 3                      | 20.73% | 34.74%   | 44.29%     | 55.40%      |
| 3                    | 3                      | 0.00%  | 0.00%    | 0.00%      | 0.00%       |

The EER is considered best at 0.00% and a rise in the EER indicates worse performance (Dunstone & Yager, 2009). Table 4.32 shows that the highest performance was found when matching condition 3 to condition 3. This scenario had an EER of 0.00%. This was the only matching scenario with a perfect EER. When matching images from condition 3 against images from condition 3, Megamatcher was able to differentiate all of the genuine attempts from the impostor attempts. Condition 1 vs condition 1 had an EER of 3.93%, condition 1 vs condition 3 had an EER of 3.15%, and condition 2a vs condition 2a had an EER of 0.90%. While the three previously mentioned scenarios do not perform perfectly, they do show that matching across the listed conditions is possible. The remaining scenarios did not perform well. The DET curves for the nine different matching scenarios can be found in Appendix B.

The operational significance of matching condition 1 to condition 3 is interesting. The performance of matching condition 1 to condition 3 shows that a positive match can be made

when the first image is taken before vitreous is removed and the second image is taken when the vitreous is replaced by saline. This shows that significant damage does not occur when the vitreous is removed. It also shows that the patterns of the iris are preserved when vitreous is sampled and then saline is injected into the eye.

## CHAPTER 5. CONCLUSIONS AND FUTURE WORK

This study explored the use of iris recognition on the post-mortem eye with captures at three different settings. Some research has examined the suitability of the post-mortem iris for recognition (Sauerwein et al., 2017; Trokielewicz et al., 2016, 2019), but no research had previously examined post-mortem iris recognition with multiple conditions of the eye.

### 5.1 Conclusions

The results of this work showed that the condition of the eye at the time of the post-mortem capture does affect both the image quality as well as the matching performance. Images captured at condition 2b, when the eye was visibly deflated, had the worst image quality and performed the worst. The post-mortem iris can provide a high-quality sample when the eye is not deflated. Current matching software is able to match the templates of post-mortem irises at different conditions as well.

Some challenges were unable to be controlled for this study. Due to the operational nature of the coroner's offices, controlling the volume of vitreous that was removed from the eye was not a possibility. This meant that there was high variability during condition 2 which led to condition 2 being split into two conditions. The volume of saline solution that was injected into the eye was also uncontrolled.

#### 5.1.1 Image Quality

Suitable iris images can be captured at all four analyzed conditions. The analysis of variance of image quality scores shows that images captured from conditions 1 and 3 have higher image quality than images captured from condition 2a and 2b. Condition 2b also had a significantly worse average image quality score than condition 2a. Images from condition 2b had the worst scores for the iris detection confidence, the iris-pupil contrast, the iris radius, the pupil boundary circularity, and the usable iris area. The scores of the pupil boundary circularity showed that condition 2a was significantly lower than the scores of conditions 1 and 3.

The metrics that showed no difference among all of the conditions were the pupil concentricity, iris-sclera contrast, margin adequacy, pupil to iris ratio, and the sharpness. Between conditions 1 and 3, none of the image quality metrics showed significant differences.

The image quality analysis indicates that iris images to be used for identification should be captured at condition 1 or condition 3 because there were no significant differences found between the two conditions. If it is not possible to collect images from an eye before vitreous is removed, then the eye should be filled with saline, instead of being left deflated. An image captured from condition 2, whether it is visibly deflated or not, is likely to have worse quality than if the eye is inflated with saline solution.

### 5.1.2 Performance

The performance results showed that matching images when the vitreous is removed from the eye resulted in poor performance. The best matching performance came from images when the vitreous was replaced with a saline solution. The DET curve for the scenario matching condition 3 to condition 3 showed an EER rate of 0.00%, which is desirable performance. The performance when matching conditions 1 to 1, conditions 1 to 3, and condition 2a to 2a were acceptable, with EER's of 3.93%, 3.15%, and 0.90% respectively. This showed that the system was able to distinguish most genuine attempts from impostor attempts at those matching scenarios. The remaining matching scenarios involving conditions 2a and 2b performed undesirably.

The performance results indicate that iris images should be captured when the volume of the vitreous humor is normal. If the eye has not lost any vitreous fluid, then a capture can be attempted. In the event that vitreous fluid had been previously been sampled or a loss of vitreous occurred from other means, saline solution should be injected into the eye to restore the shape of the eye before a capture is attempted.

## 5.2 Future Work

During the completion of this research, additional questions came to fruition. The following recommendations could be used in future replications of this study.

1. Capturing images from users before and after death will need to be investigated. This would determine if the pattern of the iris change after death.
2. Increasing the number of subjects and range of subject demographics would be useful.
3. Additional conditions of post-mortem iris captures can be investigated. The following conditions are suggested:
  1. Before any procedures are performed on the eye, including the use of saline to rinse the eye.
  2. After the eye has been flushed clean with saline.
  3. After the vitreous has been sampled from the eye.
  4. With a volume of saline used to replace the sampled vitreous.
4. It could be useful to standardize the volume of vitreous sampled from each eye and the volume of saline used to replace the vitreous.
5. Determining how different volumes of sampled vitreous affect the ability to recognize an iris would be useful.
6. The demographic information collected should consist of more variables including but not limited to the time of death, a more detailed reporting of the cause of death, and pre-existing medical conditions of the eye.
7. Additional capture devices should be tested. The only device used was the IriShield USB MK2120U. Further studies can be conducted to determine if other devices perform similarly.
8. Additional matching software should be tested. The only matching algorithm used was Neurotechnology SDK 10. Further studies can be conducted to determine if other software performs similarly.

# APPENDIX A. INSTITUTIONAL REVIEW BOARD EXEMPTION



HUMAN RESEARCH PROTECTION PROGRAM  
INSTITUTIONAL REVIEW BOARDS

---

**To:** STEPHEN J. ELLIOTT

**From:** INSTITUTIONAL REVIEW BOARD  
YONG

**Date:** 05/13/2019

**Committee Action:** **IRB Review Not Required**

**IRB Protocol #:** 1905022117

**Study Title:** Post Mortem Iris Recognition

Thank you for your submission. We have reviewed the above-referenced project and determined that it does not meet the definition of human subjects research as defined by 45 CFR 46. Consequently, it does not require IRB review. If the project changes scope such that it may become human subjects research in the future, please contact us.

You are required to retain a copy of this letter for your records. We appreciate your commitment towards ensuring the ethical conduct of human subjects research and wish you luck with your project.

---

Ernest C. Young Hall, 10th Floor - 155 S. Grant St. - West Lafayette, IN 47907-2114 - (765) 494-5942 - Fax: (765) 494-9911

Figure A 1: IRB Human Subjects Research Exemption

## APPENDIX B. PERFORMANCE DET CURVES

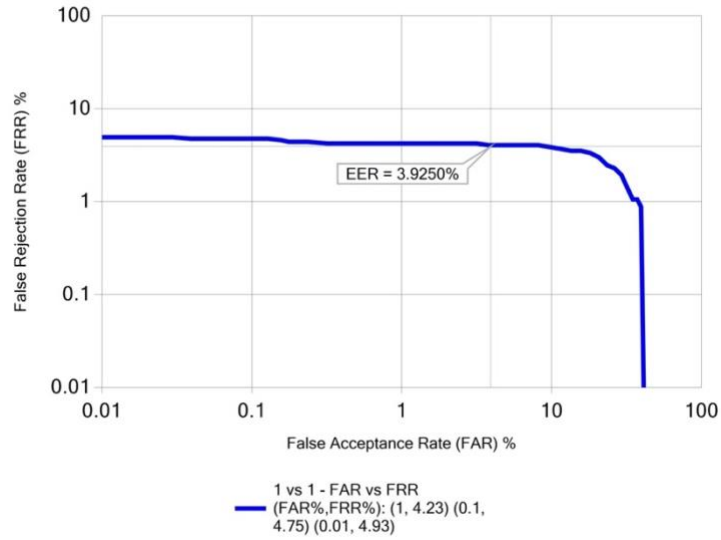


Figure B 1: DET Curve: Condition 1 vs Condition 1

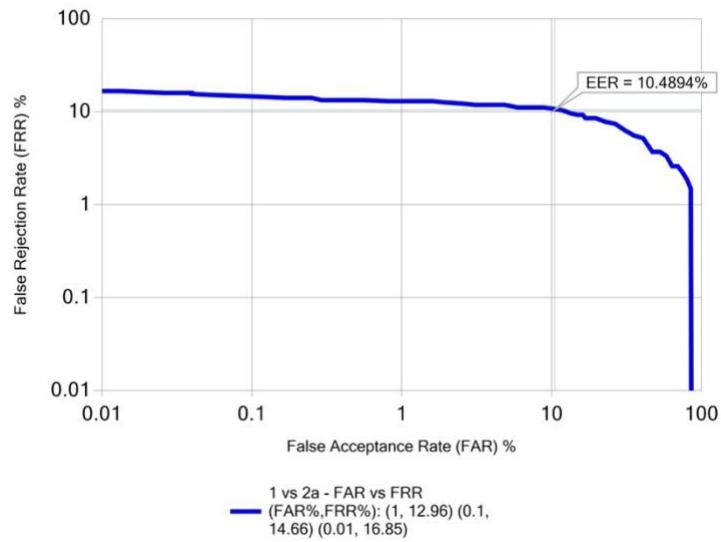


Figure B 2: DET Curve: Condition 1 vs Condition 2a

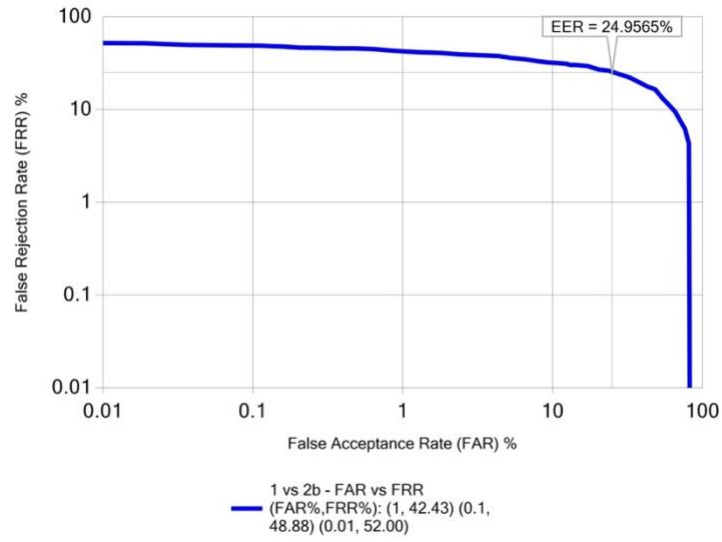


Figure B 3: DET Curve: Condition 1 vs Condition 2b

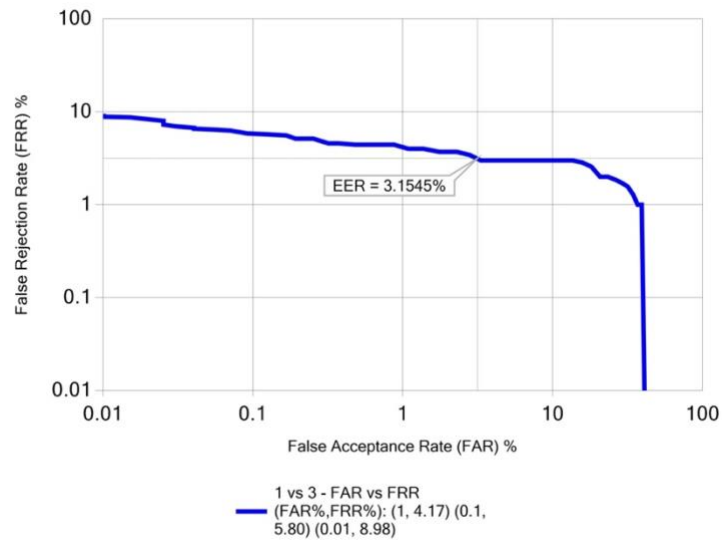


Figure B 4: DET Curve: Condition 1 vs Condition 3

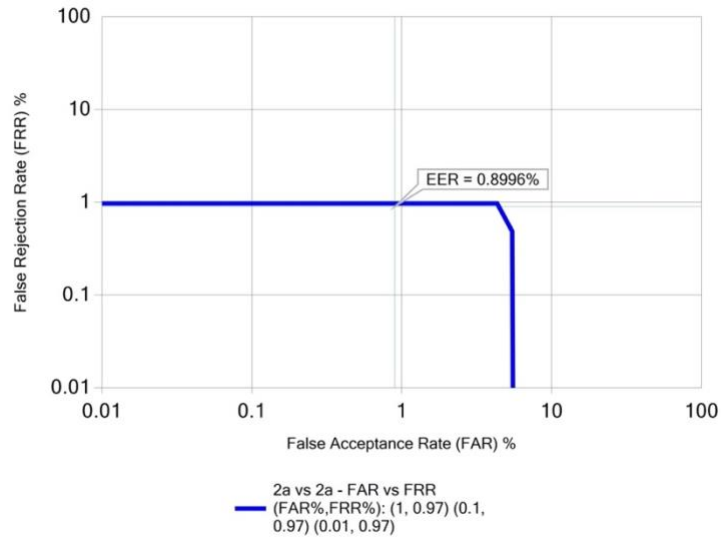


Figure B 5: DET Curve: Condition 2a vs Condition 2a

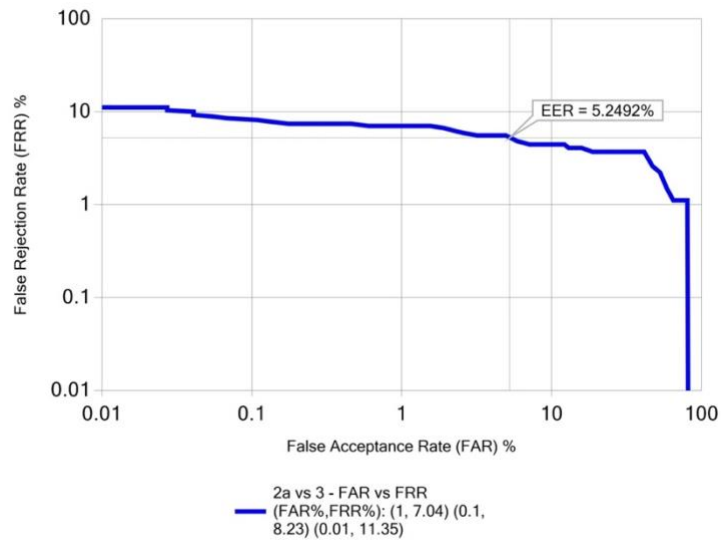


Figure B 6: DET Curve: Condition 2a vs Condition 3

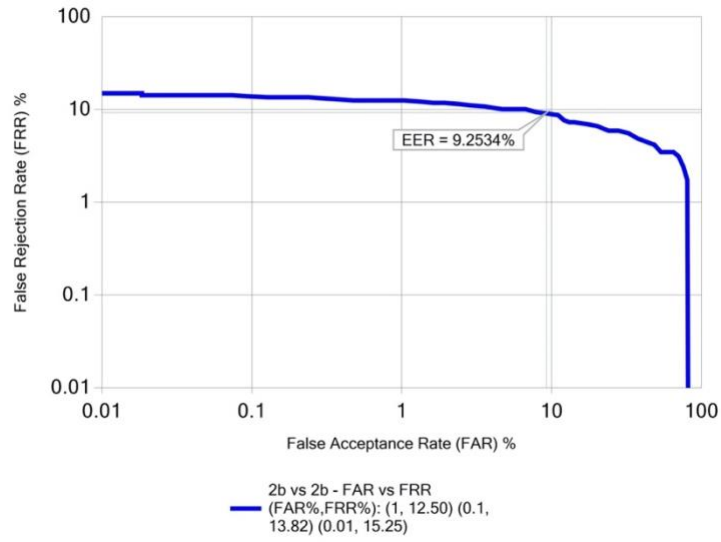


Figure B 7: DET Curve: Condition 2b vs Condition 2b

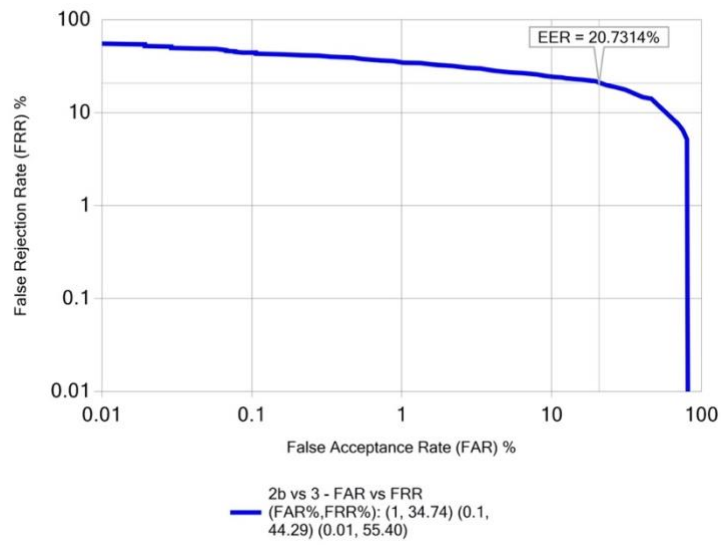


Figure B 8: DET Curve: Condition 2b vs Condition 3

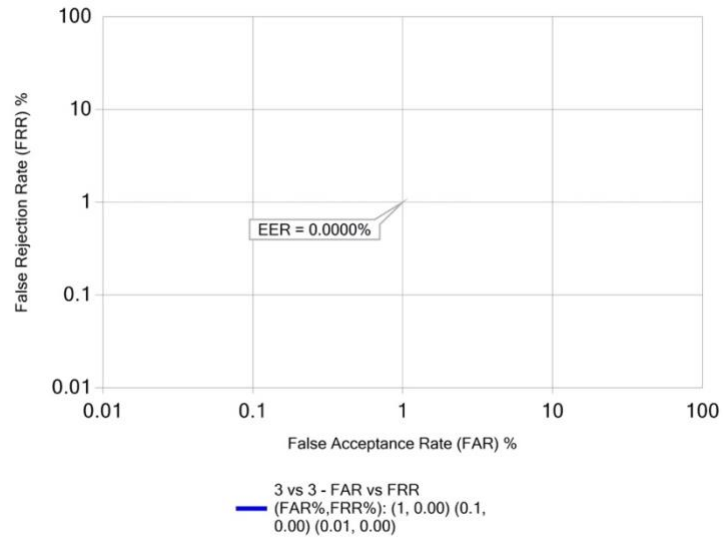


Figure B 9: DET Curve: Condition 3 vs Condition 3

## REFERENCES

- Al-Raisi, A. N., & Al-Khoury, A. M. (2008). Iris recognition and the challenge of homeland and border control security in UAE. *Telematics and Informatics*, 25(2), 117–132.  
doi:10.1016/j.tele.2006.06.005
- American Society of Retina Specialists. (2016). Vitrectomy - The American Society of Retina Specialists. Retrieved November 19, 2019, from <https://www.asrs.org/patients/retinal-diseases/25/vitrectomy>
- Atkins, E. J., Newman, N. J., & Biousse, V. (2008). Post-traumatic visual loss. *Reviews in Neurological Diseases*, 5(2), 73–81.
- BBC News. (2001, August 9). The eyes have it. Retrieved March 18, 2019, from <http://news.bbc.co.uk/2/hi/science/nature/1477655.stm>
- Bergmuller, T., Debiasi, L., Uhl, A., & Sun, Z. (2014). Impact of sensor ageing on iris recognition. In *IEEE International Joint Conference on Biometrics* (pp. 1–8). IEEE.  
doi:10.1109/BTAS.2014.6996274
- Bévalot, F., Cartiser, N., Bottinelli, C., Fanton, L., & Guitton, J. (2016). Vitreous humor analysis for the detection of xenobiotics in forensic toxicology: a review. *Forensic Toxicology*, 34, 12–40. doi:10.1007/s11419-015-0294-5
- Bowyer, K. W., Hollingsworth, K. P., & Flynn, P. J. (2016). A survey of iris biometrics research: 2008–2010. In K. W. Bowyer & M. J. Burge (Eds.), *Handbook of iris recognition* (pp. 23–61). London: Springer London. doi:10.1007/978-1-4471-6784-6\_2
- Collins. (2019). Saline solution definition and meaning | Collins English Dictionary. Retrieved November 4, 2019, from <https://www.collinsdictionary.com/us/dictionary/english/saline-solution>
- Daugman, J. (1994, March 1). Biometric Personal Identification System Based on Iris Analysis. United States.
- Daugman, J. (2009). How iris recognition works. In *The essential guide to image processing* (pp. 715–739). Elsevier. doi:10.1016/B978-0-12-374457-9.00025-1
- Doggart, J. (1949). *Ocular Signs in Slit-Lamp Microscopy*. Great Britain: The C. V. Mosby Company.

- Du, Y. E. (2006). Review of iris recognition: cameras, systems, and their applications. *Sensor Review*, 26(1), 66–69. doi:10.1108/02602280610640706
- Dunstone, T., & Yager, N. (2009). *Biometric system and data analysis: Design, evaluation, and data mining*. New York: Springer.
- Flom, L., & Safir, A. (1987, February 3). Iris Recognition System. 1903 Post Rd., Fairfield, Conn. 10403.
- Frost. (2017). *Insight on Commercial Biometrics*. (Sullivan, Trans.). Frost & Sullivan Market Insight.
- Garhart, C., & Lakshminarayanan, V. (2016). Anatomy of the eye. In J. Chen, W. Cranton, & M. Fihn (Eds.), *Handbook of visual display technology* (pp. 93–104). Cham: Springer International Publishing. doi:10.1007/978-3-319-14346-0\_4
- Geberth, V. J. (2006). *Practical Homicide Investigation: Tactics, Procedures, and Forensic Technologies, Fourth Edition* (4th ed., p. 1072). Boca Raton, FL: Taylor & Francis, Inc.
- International Standard Organization. (2017). Information Technology - Vocabulary - Part 37: Biometrics. *ISO/IEC 2382-37*.
- Jain, A. K., Ross, A., & Prabhakar, S. (2004). An introduction to biometric recognition. *IEEE Transactions on Circuits and Systems for Video Technology*, 14(1), 4–20. doi:10.1109/TCSVT.2003.818349
- James, S. H., Nordby, J. J., & Bell, S. (2014). *Forensic Science: An Introduction To Scientific And Investigative Techniques, Fourth Edition* (4th ed., p. 614). Boca Raton, Florida: Crc Press.
- JTC 1/SC 37. (2005). Information technology - Biometric data interchange formats - Part 6: Iris image data.
- Katsuhiko Hatake, W. K. (2014). Estimating the Time after Death on the Basis of Corneal Opacity. *Journal of Forensic Research*, 06(01). doi:10.4172/2157-7145.1000269
- Lund-Andersen, H., Sebag, J., Sander, B., & La Cour, M. (2005). The Vitreous. In *The biology of the eye* (Vol. 10, pp. 181–194). Elsevier. doi:10.1016/S1569-2590(05)10007-X
- Neurotechnology. (2019, January 7). Press Release: MegaMatcher 11 Product Line release. Retrieved November 30, 2019, from [https://www.neurotechnology.com/press\\_release\\_megamatcher\\_11\\_0.html](https://www.neurotechnology.com/press_release_megamatcher_11_0.html)
- Petry, B. (2015, May). *The Stability of the Iris as a Biometric Modality* (Master thesis).

- Remington, L. A. (2005). *Clinical anatomy of the visual system*. Elsevier. doi:10.1016/B978-0-7506-7490-4.X5001-7
- Rhcastilhos, & Jmarchn. (2007, January 25). Schematic diagram of the human eye en.svg - Wikimedia Commons. Retrieved October 18, 2018, from [https://commons.wikimedia.org/wiki/File:Schematic\\_diagram\\_of\\_the\\_human\\_eye\\_en.svg](https://commons.wikimedia.org/wiki/File:Schematic_diagram_of_the_human_eye_en.svg)
- Rzemyk, T. J. (2017). Biometrics in the criminal justice system and society today. In *Effective Physical Security* (pp. 249–254). Elsevier. doi:10.1016/B978-0-12-804462-9.00010-5
- Sauerwein, K., Saul, T. B., Steadman, D. W., & Boehnen, C. B. (2017). The effect of decomposition on the efficacy of biometrics for positive identification. *Journal of Forensic Sciences*, 62(6), 1599–1602. doi:10.1111/1556-4029.13484
- Skelton, D. T., Marsh, H. L., & Woods, D. D. (Eds.). (2001). *Guidebook for Indiana Coroners* (7th ed.).
- Stracener, J. T., Matey, J. R., Faddis, K. N., & Maxey, J. R. (2013). Performance assessments of iris recognition in tactical biometric devices. *IET Biometrics*, 2(3), 107–116. doi:10.1049/iet-bmt.2012.0078
- Suvarna, S. K. (Ed.). (2016). *Atlas of adult autopsy*. Cham: Springer International Publishing. doi:10.1007/978-3-319-27022-7
- Tabassi, E., Grother, P., & Salamon, W. (2011). *Iris Quality Calibration and Evaluation*. National Institute of Standards and Technology.
- The United States Department of Justice. (2019, September 24). Forensic Science. Retrieved November 3, 2019, from <https://www.justice.gov/olp/forensic-science>
- Trokielewicz, M., & Czajka, A. (2018). Data-driven segmentation of post-mortem iris images. In *2018 International Workshop on Biometrics and Forensics (IWBF)* (pp. 1–7). IEEE. doi:10.1109/IWBF.2018.8401558
- Trokielewicz, M., Czajka, A., & Maciejewicz, P. (2016). Post-mortem Human Iris Recognition. Presented at the 9th IAPR International Conference on Biometrics (ICB 2016), Mateusz Trokielewicz.
- Trokielewicz, M., Czajka, A., & Maciejewicz, P. (2019). Iris recognition after death. *IEEE Transactions on Information Forensics and Security*, 14(6), 1501–1514. doi:10.1109/TIFS.2018.2881671

- Wayman, J. (1997). A generalized biometric identification system model. In *Conference Record of the Thirty-First Asilomar Conference on Signals, Systems and Computers (Cat. No.97CB36136)* (pp. 291–295). IEEE Comput. Soc. doi:10.1109/ACSSC.1997.680201
- Winn, B., Whitaker, D., Elliott, D. B., & Phillips, N. J. (1994). Factors affecting light-adapted pupil size in normal human subjects. *Investigative Ophthalmology & Visual Science*, 35(3), 1132–1137.